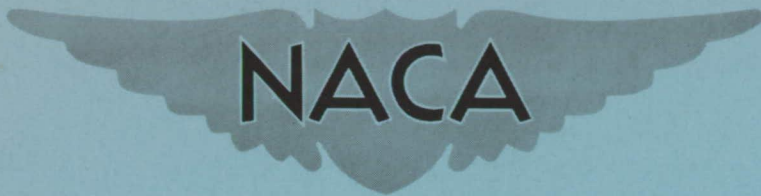


**CONFIDENTIAL**

Copy  
RM L54I07a



# RESEARCH MEMORANDUM

AN EXPERIMENTAL TRANSONIC INVESTIGATION OF A  
45° SWEPTBACK WING-BODY COMBINATION WITH  
SEVERAL TYPES OF BODY INDENTATION WITH  
THEORETICAL COMPARISONS INCLUDED

By Melvin M. Carmel

Langley Aeronautical Laboratory  
Langley Field, Va.

*Classification Changed to Unclassified  
Authority: NASA Technical Publications  
Announcement No. 8  
Effective Date: July 22, 1959*  
WHL

CLASSIFIED DOCUMENT

This material contains information affecting the National Defense of the United States within the meaning of the espionage laws, Title 18, U.S.C., Secs. 793 and 794, the transmission or revelation of which in any manner to an unauthorized person is prohibited by law.

## NATIONAL ADVISORY COMMITTEE FOR AERONAUTICS

WASHINGTON

November 19, 1954

**CONFIDENTIAL**

## NATIONAL ADVISORY COMMITTEE FOR AERONAUTICS

## RESEARCH MEMORANDUM

## AN EXPERIMENTAL TRANSONIC INVESTIGATION OF A

## 45° SWEEPBACK WING-BODY COMBINATION WITH

## SEVERAL TYPES OF BODY INDENTATION WITH

## THEORETICAL COMPARISONS INCLUDED

By Melvin M. Carmel

## SUMMARY

An investigation has been made to determine the effects of several types of body indentation on the transonic aerodynamic characteristics of a 45° sweptback wing-body combination. The wing had an aspect ratio of 4 and a taper ratio of 0.3. The results were obtained in the Langley 8-foot transonic tunnel at Mach numbers from 0.80 to 1.15, angles of attack from 0° to 12°, and Reynolds numbers based on the mean aerodynamic chord of the wing from  $1.80 \times 10^6$  to  $2.00 \times 10^6$ .

The results of this investigation show that partial indentation, of the order of half that needed to satisfy the transonic area rule, leads to considerable reduction in the zero-lift drag-rise coefficient at sonic and low supersonic speeds. This reduction in the drag-rise coefficient is somewhat more than proportional to the amount of cross-sectional area removed from the wing-body combination. For partially indented configurations such as those of this test, the zero-lift drag-rise coefficient near a Mach number of 1.00 is primarily dependent upon the amount of cross-sectional area removed and not dependent upon the location on the periphery of the body at which the area is removed. Increasing the slope of the body indentation near the leading edge of the wing up to twice that used to conform with the transonic area rule has little effect on the incremental drag due to lift at a lift coefficient of 0.3 for the combination. This type of modification, however, increases the zero-lift drag-rise coefficients near a Mach number of 1.00 above those obtained with the combination incorporating normal indentation. Deviations from body indentation in accordance with the transonic area rule such as those of this test lowered the maximum lift-drag ratios in the supercritical Mach number range up to at least a Mach number of 1.15. Zero-lift drag-rise coefficients for the wing-body combinations such as those of this investigation cannot be calculated accurately at sonic speed, but can be computed with a considerable degree of accuracy at low supersonic Mach numbers of the order of 1.20.

## INTRODUCTION

Numerous investigations have been performed to show that body modification based on the transonic area rule of reference 1 will result in considerable drag reduction near sonic speed. These investigations (such as those of refs. 2, 3, and 4) consisted of symmetrically indenting a wing-body combination so that the axial cross-sectional area of the combination was equal to that for the body alone. In the application of the area rule to body indentation, a number of solutions to problems concerning possible variations in indentation methods are required to help determine the scope and the limitations of the transonic area rule. Among the problems to be solved are the following: If a fuselage cannot be fully indented because of necessary equipment space, what will be the effect of partial indentation? What is the relative effect of indentation on the sides of a body rather than equal indentation all around a body? In order to investigate these problems, a sweptback wing-body combination was indented so that only half of the axial cross-sectional area of the wing was removed from the body. This same combination was then indented so that the indentation in the plane of the wing was a normal indentation, and this indentation elliptically approached zero at the top and bottom of the body.

Another factor that enters into this investigation is that of symmetrical modification or asymmetrical modification to body indentation either above or below the wing. The results of reference 5 showed that, with twice the slope of the normal body indentation near the wing leading edge either above or below the wing, there was an appreciable reduction in drag due to lift near sonic speed. Since either modification was beneficial, it was believed that a symmetrical modification to the indentation would also be of benefit at lifting conditions. An indented, sweptback wing-body combination was therefore symmetrically modified so that the slope of the indentation near the leading edge of the wing was doubled. In order to simulate the area distribution for the tests of reference 5, another symmetrical modification, only half again the initial slope of that for the indented combination, was made to the indentation. Since the present wing-body combination was different from that for the investigation of reference 5, asymmetrical indentations above and below the wing plane were also tested in order to have a more valid comparison of the results.

Recently a method of computing drag-rise coefficients based on linearized theory was brought out in reference 6. This method, in essence, was used to calculate the drag-rise coefficients based on the slopes of area distribution curves for a wing-body-tail combination. In order to provide further comparisons between experiment and this theory, the slopes of the area distributions for the wing-body combinations of the present investigation were computed, and the drag-rise coefficients based on the computational methods of reference 6 were obtained.

The investigation was made in the Langley 8-foot transonic tunnel. Data were obtained at Mach numbers from 0.80 to 1.15, angles of attack from  $0^\circ$  to  $12^\circ$ , and Reynolds numbers based on the mean aerodynamic chord of the wing from  $1.80 \times 10^6$  to  $2.00 \times 10^6$ .

## SYMBOLS

$\bar{c}$	mean aerodynamic chord, in.
$C_D$	drag coefficient based on wing area of 1 square foot
$\Delta C_{D_0}$	zero-lift drag-rise coefficient, incremental drag between the drag at Mach number 0.80 and any higher Mach number
$C_L$	lift coefficient based on wing area of 1 square foot
$C_m$	pitching-moment coefficient about 0.25-chord point of $\bar{c}$
$D$	drag, lb
$L$	lift, lb
$(L/D)_{\max}$	maximum lift-drag ratio
$l$	length of body, in.
$M$	Mach number
$\alpha$	angle of attack, deg
$p$	static pressure just inside base of model, lb/sq ft
$p_0$	free-stream static pressure, lb/sq ft
$q$	free-stream dynamic pressure, $0.7p_0M^2$ , lb/sq ft
$P_b$	base pressure coefficient, $\frac{p - p_0}{q}$
$S_w$	wing area, sq ft
$ds/dX$	first derivative of the projected cross-sectional area with respect to $X$
$X$	axial distance from nose, in.

$\theta$  complement of the angle between Z axis and intersection of cutting planes with YZ plane, deg (see ref. 6)

$$\phi = \arccos \frac{1 - 2X}{7}$$

## APPARATUS AND METHODS

### Tunnel

The tests were conducted in the Langley 8-foot transonic tunnel which is a dodecagonal, single-return, slotted wind tunnel (see ref. 7). This tunnel operates at atmospheric stagnation pressures.

### Configurations

The test wing has  $45^\circ$  sweepback of the 0.25-chord line, an aspect ratio of 4, a taper ratio of 0.3, and NACA 65A006 airfoil sections parallel to the model plane of symmetry. This wing is the same as the low-taper-ratio wing of reference 2. The boattail body used for these tests is also the same as that used for the tests of reference 2. The outer part of the body in the axial location of the wing was made of detachable, wood-impregnated plastic, thus facilitating the manufacture and the installation of the various indented bodies for this investigation. Dimensional details for the basic wing-body combination may be found in figure 1. Cross-sectional views of the various indented bodies at two axial stations may be found in figure 2. Table 1 gives the coordinates for the various indented bodies tested; and the axial cross-sectional area distribution, together with that for the wing, may be found in figure 3. For the sake of clarity in this report, the indentation made in accordance with the transonic area rule is called "normal." The indentation with one-half of the normal indentation is called "partial." With partial indentation such that the indentation in the plane of the wing is a normal indentation and elliptically approaches zero at the top and the bottom of the body, the indentation is identified as "side." This combination has the same axial area distribution as the partial-indentation combination. With the forward part of the indentation doubled in slope, the indentation is called "deep, rapid." With the forward slope of the indentation half again as large as that for the normal indentation, the indentation is called "moderate, rapid." With the normal indentation on the top of the body and the deep, rapid indentation on the bottom of the body (the wing being considered as the plane of symmetry), the indentation is called "lower, rapid." With these latter two indentations reversed, the indentation is called "upper, rapid." Coordinates for these latter two configurations are obtained from combinations of coordinates for the deep, rapid indentation and the normal indentation of reference 2.

The model was attached to the forward end of an enclosed electrical strain-gage balance. This balance was attached by means of a sting to the tunnel central support system. The model was offset from the center line of the tunnel.

### Measurements and Accuracy

The average free-stream Mach number was determined to within  $\pm 0.003$  by a calibration with respect to the pressure in the chamber surrounding the slotted test section. Deviations from the average free-stream Mach number in the model test region were of the order of 0.003 at subsonic speeds and increased to as much as 0.01 at a Mach number of 1.13.

The accuracy of the lift, drag, and pitching-moment coefficients, based on balance calibrations and reproducibility of the data, is believed to be within  $\pm 0.01$ ,  $\pm 0.001$ , and  $\pm 0.002$ , respectively.

The drag data have been adjusted for base pressure so that the drag corresponds to conditions for which the body base pressure would be equal to the free-stream static pressure. The base-pressure coefficients obtained from these tests may be found in figure 4. Base pressures were measured by means of a ring of static orifices located 0.5 inch within the base of the body.

Tests were not performed between Mach numbers of 1.03 and 1.15, except for the asymmetrical, rapidly indented combinations, because of tunnel-wall interference which consisted of boundary-reflected disturbances (ref. 7). On all cross-plotted data, however, these two Mach numbers were connected with an arbitrary fairing. For the asymmetrical combinations, because of power limitations, tests were performed and data are presented at a Mach number of 1.13. These data are known to contain some inaccuracies; however, they should offer qualitative trends for comparison with other data presented. Some of the data could not be obtained for as high lift coefficients as other data because of excessively high balance loads.

The angle of attack of the model was measured by a pendulum-type accelerometer-inclinometer mounted in the model nose. The accuracy of this device is estimated to be within  $\pm 0.1^\circ$ .

### RESULTS AND DISCUSSION

The basic aerodynamic characteristics (angle of attack, drag coefficient, and pitching-moment coefficient about the 0.25 chord of the mean aerodynamic chord) plotted against lift coefficient for the various indented, sweptback wing-body combinations tested are presented in

figures 5 to 10. The aerodynamic characteristics for the basic combination and the combination indented in accordance with the transonic area rule may be found in reference 2.

### Drag Characteristics

Partial indentation.- The effect on the zero-lift drag-rise coefficient of partial indentation on a wing-body combination is shown in figure 11. As previously mentioned, this indentation consisted of indenting the body only half as much as that needed to satisfy the transonic area rule. It may be seen in figure 11 that, at a Mach number of 1.00, the combination with the normal (transonic-area-rule) indentation has a reduction in zero-lift drag-rise coefficient of 76 percent as compared with the drag-rise coefficient for the basic wing-body combination. Partial body indentation also leads to a substantial reduction in the zero-lift drag-rise coefficient at sonic speed, and for this condition, the reduction in the zero-lift drag-rise coefficient is 61 percent of that achieved with normal indentation. Thus, it is shown that reduction in the zero-lift drag-rise coefficient due to partial indentation is somewhat more than proportional to the amount of cross-sectional area removed from the wing-body combination. At the highest test Mach number of 1.15, partial indentation leads to a reduction in the zero-lift drag-rise coefficient of 74 percent of that achieved with normal indentation. These data therefore indicate that, for practical aircraft for which incorporation of normal indentation may be impossible, substantial reductions in the zero-lift drag-rise coefficients may be obtained by partial indentation, not only at sonic speed but also in the lower supersonic Mach number range.

Side indentation.- The zero-lift drag-rise coefficients of the combination with side indentation are plotted against Mach number in figure 12. Since the axial cross-sectional area of the partially indented combination was the same as that for the combination with side indentation, the zero-lift drag-rise coefficients for this combination were used for comparative purposes. It may be seen from figure 12 that the zero-lift drag-rise coefficients are essentially the same at all test Mach numbers for wing-body combinations with these two indentations. This result indicates that, for a practical aircraft configuration at sonic or very low supersonic speeds, partial indentations on only the sides of the fuselage may result in drag-rise reductions of the same order of magnitude as those obtained with corresponding indentation all around the body.

Rapid indentations.- The effect on the drag coefficient of increasing the forward slope of the normal indentation of the body is shown in figure 13. It may be seen that, at zero lift, there are small differences in subcritical drag coefficients for the combinations presented, but these differences are believed to be due to almost unnoticeable differences in roughness of the combinations during the tests. Reference 8 has shown

that, with almost unnoticeable changes of roughness on a wing surface, the position of flow transition will change and result in a drag increment for a wing-body combination of the types tested herein. Drag changes caused by this type of phenomenon should be minimized at moderate lifting conditions, since with increasing angle of attack, the position of the transition for a wing moves forward in the same manner as that caused by increased surface roughness, so that the position of flow transition is equalized for either rough or smooth wing surfaces. It may be seen from figure 13 that, near a Mach number of 1.00, any of the more rapidly indented combinations generally lead to higher drag coefficients, up to lift coefficients of 0.5, than does the normally indented combination.

Figure 14 shows that the zero-lift drag-rise coefficient of the configuration with normal indentation near a Mach number of 1.00 is lower than that for any of the more rapidly indented combinations. At a Mach number of 1.15, the zero-lift drag-rise coefficients for the more rapidly indented combinations with indentations made all around the body are about the same as for the normally indented combination. Removing the cross-sectional area from only the top or only the bottom of the body, however, results in a somewhat lower zero-lift drag-rise coefficient at a Mach number of 1.15 than for the normally indented combination.

The curves of figure 15 show that there is little difference in the incremental drag due to lift at a lift coefficient of 0.3 for the normally indented combination and any of the more rapidly indented combinations throughout the test Mach number range, except for the combination with upper, rapid indentation near Mach numbers of 0.80 and 1.03. Near these two Mach numbers, the combination with upper, rapid indentation provides slightly lower incremental drag coefficients than does the normally indented combination.

Maximum lift-drag ratio.- The variation of maximum lift-drag ratio with Mach number for the various test combinations is shown in figure 16. The figure shows that, above a Mach number of about 0.95 to the highest test Mach number, deviations from body indentation in accordance with the transonic-area rule, such as those of this test, lower the maximum lift-drag ratios. These same deviations from normal body indentation also lead to lower Mach numbers at which the curves of maximum lift-drag ratio are sharply reduced.

These results on maximum lift-drag ratio and drag due to lift for the more rapidly indented combinations do not verify the results of similar tests presented in reference 5. The inconsistency between these data and those of reference 5 indicates that this type of body indentation is relatively dependent upon the particular aircraft used and should not be incorporated in design without considerably more study.



Comparison between experiment and theory.- As previously mentioned, a method of computing zero-lift drag-rise coefficient was recently advanced. From reference 6,

$$\Delta C_{D_0} = \frac{1}{576S_w} \left(\frac{l}{2}\right)^2 \int_0^\pi \sum_{n=1}^{n=24} n A_n^2 d\theta$$

where

$$A_1 = \frac{4}{\pi l} \int_0^\pi \frac{ds}{dX} \sin \phi d\phi$$

$$A_2 = \frac{4}{\pi l} \int_0^\pi \frac{ds}{dX} \sin 2\phi d\phi$$

.....

The theoretical computations presented herein are for Mach numbers of 1.00 and 1.20. Computations were made for Mach numbers of 1.00 and 1.20 since area distributions were available for these Mach numbers. However, the highest test Mach number obtained was only 1.15. It is believed, however, that a comparison of the experimental data at a Mach number of 1.15 with the theoretical computations of zero-lift drag-rise coefficient for a Mach number of 1.20 will afford a valid comparison of results since the computed zero-lift drag-rise coefficients of reference 6 were essentially the same between Mach numbers of 1.15 and 1.20 for the sweptback wing-body configuration. For a Mach number of 1.00, the Mach angle is  $90^\circ$ , and any value for the angle  $\theta$  will give the same area distribution and, consequently, the same slopes for the area distributions. At Mach numbers greater than 1.00, the Mach angle is less than  $90^\circ$  and different angles of  $\theta$  result in different area distributions, and different drag coefficients are associated with each of the area distributions. For the drag computations presented herein for a Mach number of 1.20, the values of  $\theta = 0^\circ, 45^\circ, 90^\circ, 135^\circ, \text{ and } 180^\circ$  are used; this range of roll angles is assumed sufficient for a tailless, essentially symmetrical model. The corresponding angles of cut across the wing are  $0^\circ, 26^\circ, 34^\circ, 26^\circ, \text{ and } 0^\circ$ . The resulting zero-lift drag-rise coefficients for the various values of  $\theta$  were numerically integrated according to the Newton-Cotes equation (eq. (8), p. 124 of ref. 9). The area-distribution plots for the various combinations for five values of  $\theta$  at a Mach number of 1.20 are presented in figures 3 and 17, and the corresponding plots for the slopes of these curves are found in figure 18. It may be noted in figures 3, 17, and 18 that the length of the body used is 41.90 inches rather than the actual length of 41.25 inches. This extension was used for computing the zero-lift drag-rise coefficient

data in order not to have a discontinuity in the slope curves and was done by adding a cusp at the aft end of the body to a slope of zero.

Figure 19 gives the experimental and theoretical zero-lift drag-rise coefficients for the various combinations tested. It may be noted from the figure that all of the theoretical values of the drag-rise coefficient at a Mach number of 1.00 are considerably higher than the corresponding experimental values. This comparison checks with the results of reference 6. One interesting point to be noted in figure 19 is that, from the theoretical drag-rise coefficient results at a Mach number of 1.00, the 50-percent-partial indentation reduces the drag-rise coefficient 68 percent of the reduction achieved by normal indentation, compared with the 61 percent of the reduction shown by experimental results. It can also be seen from figure 19 that the theoretical drag-rise coefficients at a Mach number of 1.20 are from 5 percent to 10 percent lower than the experimental results at a Mach number of 1.15. Assuming that the experimental coefficients may possibly be slightly higher at a Mach number of 1.20 than at a Mach number of 1.15, the percent differences in experimental and theoretical drag-rise coefficients would still be less than the differences shown in reference 6. In that report, the theoretical coefficients were about 20 percent less than the experimental coefficients. These differences, in the case of the tests presented herein, moreover, are close to the testing accuracies given for this investigation. These experimental and theoretical results, therefore, indicate that zero-lift drag-rise coefficients for indented wing-body configurations cannot be calculated accurately at sonic speed, but can be calculated with a considerable degree of accuracy at low supersonic Mach numbers of the order of 1.20.

### CONCLUSIONS

Tests have been performed to determine the effect of several types of body indentation on the aerodynamic characteristics of a  $45^\circ$  sweptback wing-body combination. The results of these tests lead to the following conclusions:

1. Partial indentation, of the order of half that needed to satisfy the transonic area rule, provides considerable reduction in the zero-lift drag-rise coefficient at sonic and low supersonic speeds. This reduction in the zero-lift drag-rise coefficient is somewhat more than proportional to the amount of cross-sectional area removed from the wing-body combination.

2. For configurations with partial-indentations similar to those of this investigation, the zero-lift drag-rise coefficient near a Mach number of 1.00 is primarily dependent upon the amount of cross-sectional area removed, and not upon the location on the periphery of the body at which the area is removed.

3. Increasing the slope of the body indentation, near the leading edge of the wing, up to double that used to conform with the transonic area rule has little effect on the incremental drag due to lift at a lift coefficient of 0.3 for the wing-body combination. This type of modification, however, increases the zero-lift drag-rise coefficients of a wing-body combination near a Mach number of 1.00 over that obtained with the combination incorporating normal indentation.

4. Deviations from body indentation in accordance with the transonic area rule such as those of this investigation lower the maximum lift-drag ratios in the supercritical Mach number range up to at least a Mach number of 1.15.

5. Zero-lift drag-rise coefficients for wing-body combinations such as those of this investigation cannot be calculated accurately at sonic speed, but can be calculated with a considerable degree of accuracy at low supersonic Mach numbers of the order of 1.20.

Langley Aeronautical Laboratory,  
National Advisory Committee for Aeronautics,  
Langley Field, Va., August 23, 1954.

## REFERENCES

1. Whitcomb, Richard T.: A Study of the Zero-Lift Drag-Rise Characteristics of Wing-Body Combinations Near the Speed of Sound. NACA RM L52H08, 1952.
2. Morgan, Francis G., Jr., and Carmel, Melvin M.: Transonic Wind-Tunnel Investigation of the Effects of Taper Ratio, Body Indentation, Fixed Transition, and Afterbody Shape on the Aerodynamic Characteristics of a 45° Sweptback Wing-Body Combination. NACA RM L54A15, 1954.
3. Robinson, Harold L.: A Transonic Wind-Tunnel Investigation of the Effects of Body Indentation, As Specified by the Transonic Drag-Rise Rule, on the Aerodynamic Characteristics and Flow Phenomena of a 45° Sweptback-Wing-Body Combination. NACA RM L52L12, 1953.
4. Carmel, Melvin M.: Transonic Wind-Tunnel Investigation of the Effects of Aspect Ratio, Spanwise Variations in Section Thickness Ratio, and a Body Indentation on the Aerodynamic Characteristics of a 45° Sweptback Wing-Body Combination. NACA RM L52L26b, 1953.
5. Loving, Donald L.: A Transonic Wind-Tunnel Investigation of the Effect of Modifications to an Indented Body In Combination With a 45° Sweptback Wing. NACA RM L53F02, 1953.
6. Holdaway, George H.: Comparison of Theoretical and Experimental Zero-Lift Drag-Rise Characteristics of Wing-Body-Tail Combinations Near the Speed of Sound. NACA RM A53H17, 1953.
7. Ritchie, Virgil S., and Pearson, Albin O.: Calibration of the Slotted Test Section of the Langley 8-Foot Transonic Tunnel and Preliminary Experimental Investigation of Boundary Reflected Disturbances. NACA RM L51K14, 1952.
8. Bingham, Gene J., and Braslow, Albert L.: Subsonic Investigation of Effects of Body Indentation on Zero-Lift Drag Characteristics of a 45° Sweptback Wing-Body Combination With Natural and Fixed Boundary-Layer Transition Through a Range of Reynolds Number From  $1 \times 10^6$  to  $8 \times 10^6$ . NACA RM L54B18a, 1954.
9. Milne, William Edmund: Numerical Calculus. Princeton Univ. Press, 1949.

TABLE I  
COORDINATES FOR BODIES OF TEST CONFIGURATIONS

Station, in.	Radii, in., for bodies with -			Side indentation	
	Partial indentation	Deep rapid indentation	Moderate, rapid indentation	x, in.	y, in.
0	0	0	0	0	0
.56	.19	.19	.19	a.19	a.19
1.12	.32	.32	.32	a.32	a.32
2.25	.54	.54	.54	a.54	a.54
4.50	.89	.89	.89	a.89	a.89
6.75	1.17	1.17	1.17	a1.17	a1.17
9.00	1.39	1.39	1.39	a1.39	a1.39
11.25	1.56	1.56	1.56	a1.56	a1.56
13.50	1.68	1.68	1.68	a1.68	a1.68
15.75	1.77	1.77	1.77	a1.77	a1.77
18.00	1.83	1.83	1.83	a1.83	a1.83
20.25	1.86	1.86	1.86	a1.86	a1.86
22.50	1.87	1.87	1.87	a1.87	a1.87
23.69	1.87	1.84	1.85	1.86	b1.87
24.69	1.85	1.73	1.77	1.82	b1.87
25.69	1.81	1.59	1.67	1.75	b1.87
26.69	1.77	1.51	1.59	1.66	b1.87
27.69	1.73	1.47	1.53	1.58	b1.87
28.69	1.70	1.47	1.49	1.50	b1.86
29.69	1.67	1.47	1.47	1.47	b1.85
30.69	1.66	1.47	1.47	1.47	b1.82
31.69	1.65	1.49	1.49	1.49	b1.49
32.69	1.63	1.50	1.50	1.50	b1.74
33.69	1.60	1.50	1.51	1.50	b1.69
34.69	1.57	1.50	1.50	1.50	b1.64
35.69	1.53	1.49	1.49	1.49	b1.57
36.69	1.48	1.47	1.47	1.49	b1.47
36.90	1.47	1.47	1.47	a1.47	a1.47
37.50	1.41	1.41	1.41	a1.41	a1.41
38.50	1.30	1.30	1.30	a1.30	a1.30
39.50	1.17	1.17	1.17	a1.17	a1.17
40.50	1.03	1.03	1.03	a1.03	a1.03
41.25	.94	.94	.94	a.94	a.94

<sup>a</sup>Radius.

<sup>b</sup>Major semiaxes of an ellipse.

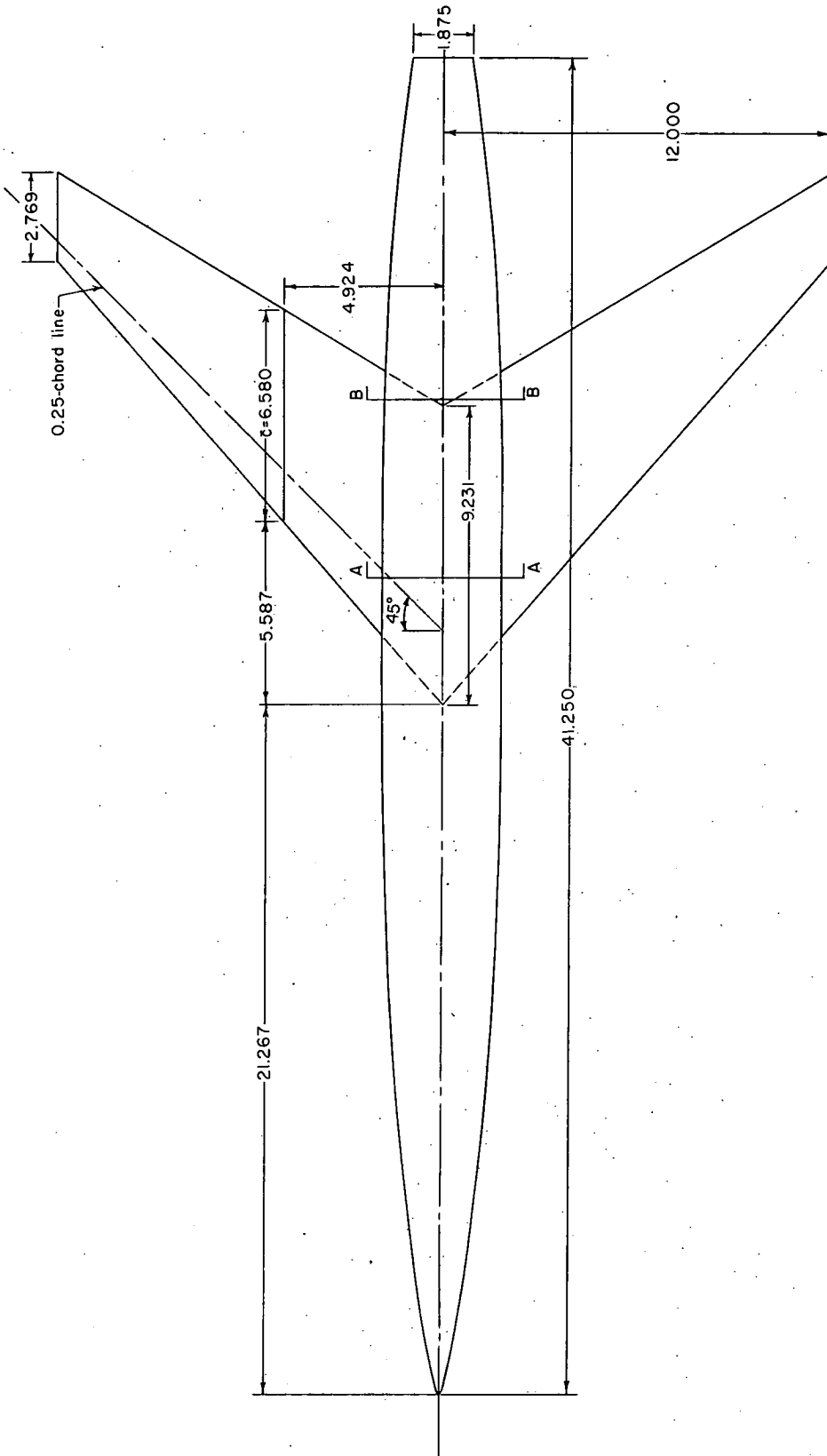
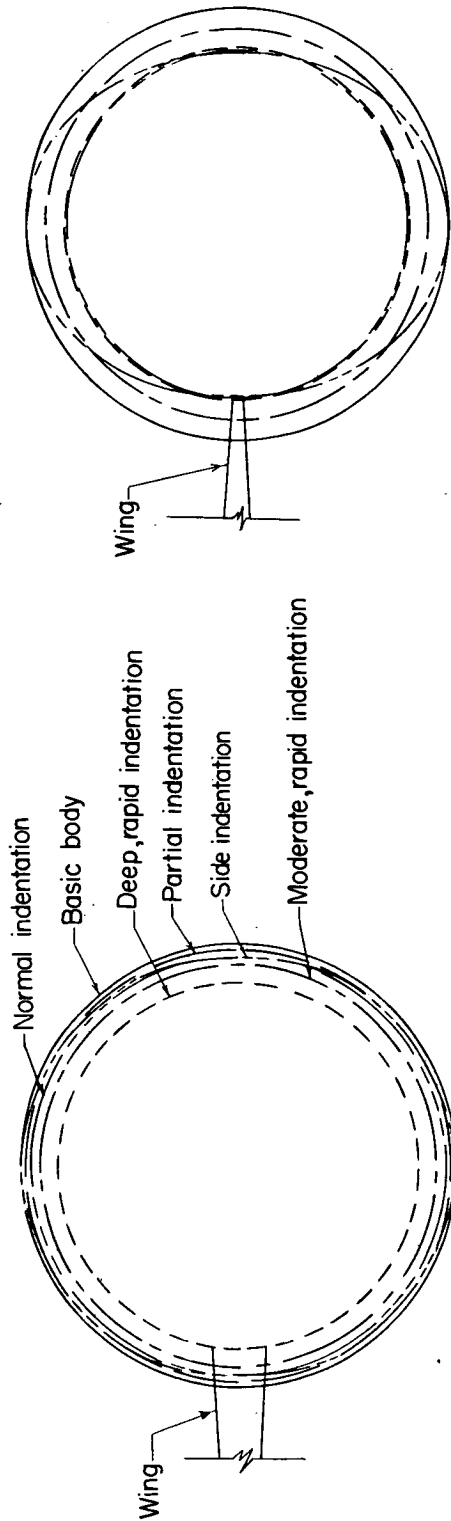


Figure 1.- Basic wing-body combination. (All dimensions are in inches.)



Station 30.692  
Section B-B

Station 25.192  
Section A-A

Figure 2.- Typical cross-sectional views of the various test bodies.  
Sections A-A and B-B are shown in figure 1.

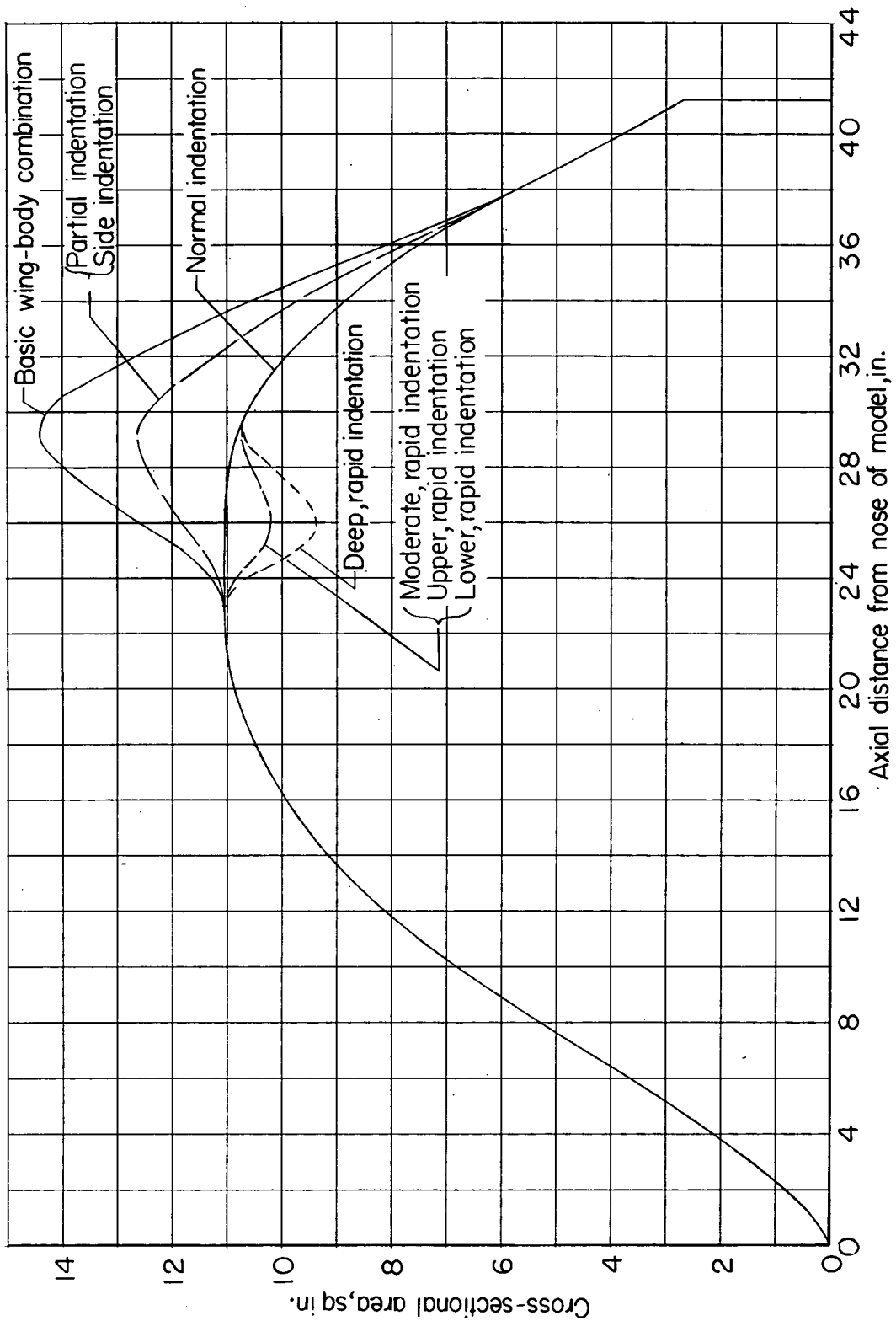
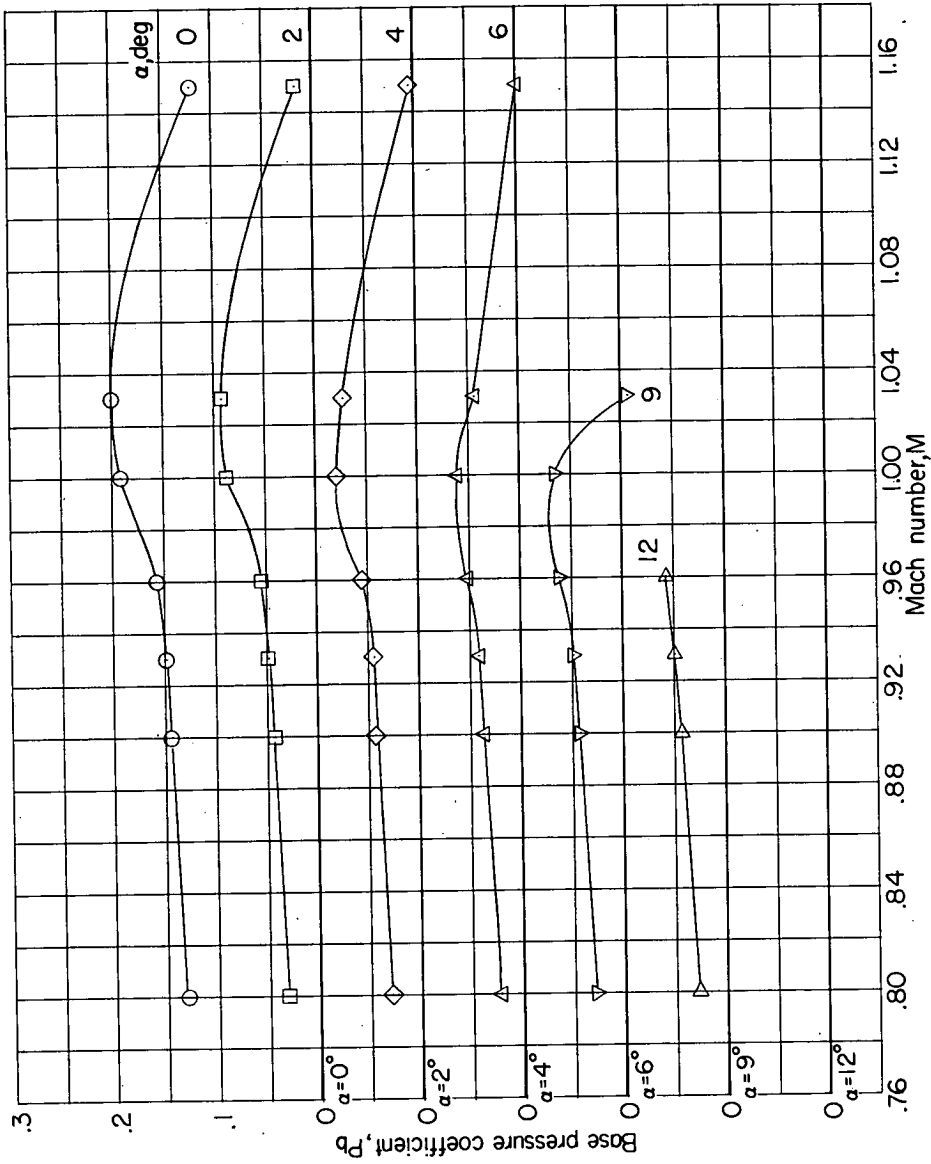


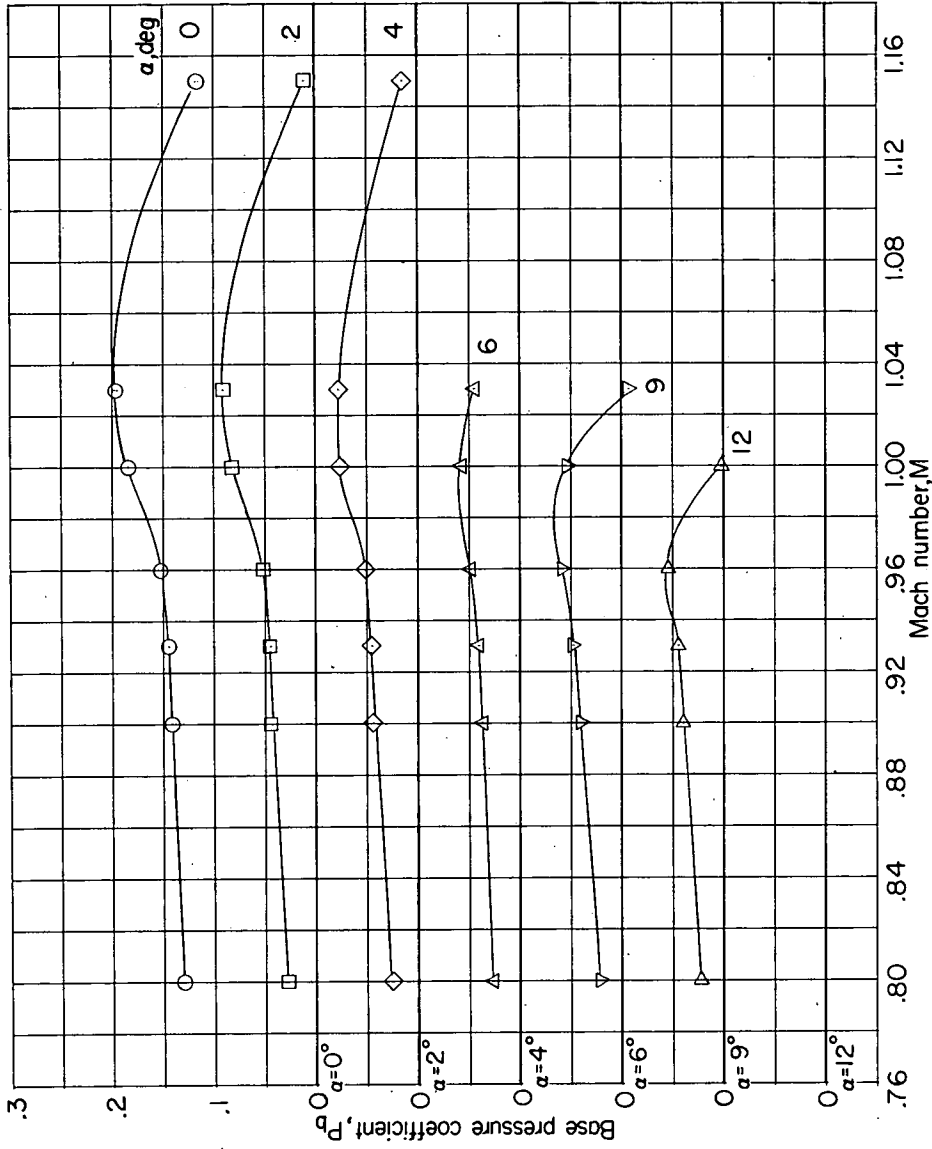
Figure 3.- Axial cross-sectional area distribution of wing-body combinations tested.  $M = 1.00$ ;  $\theta = 0^\circ$  and  $180^\circ$  for  $M = 1.20$ .





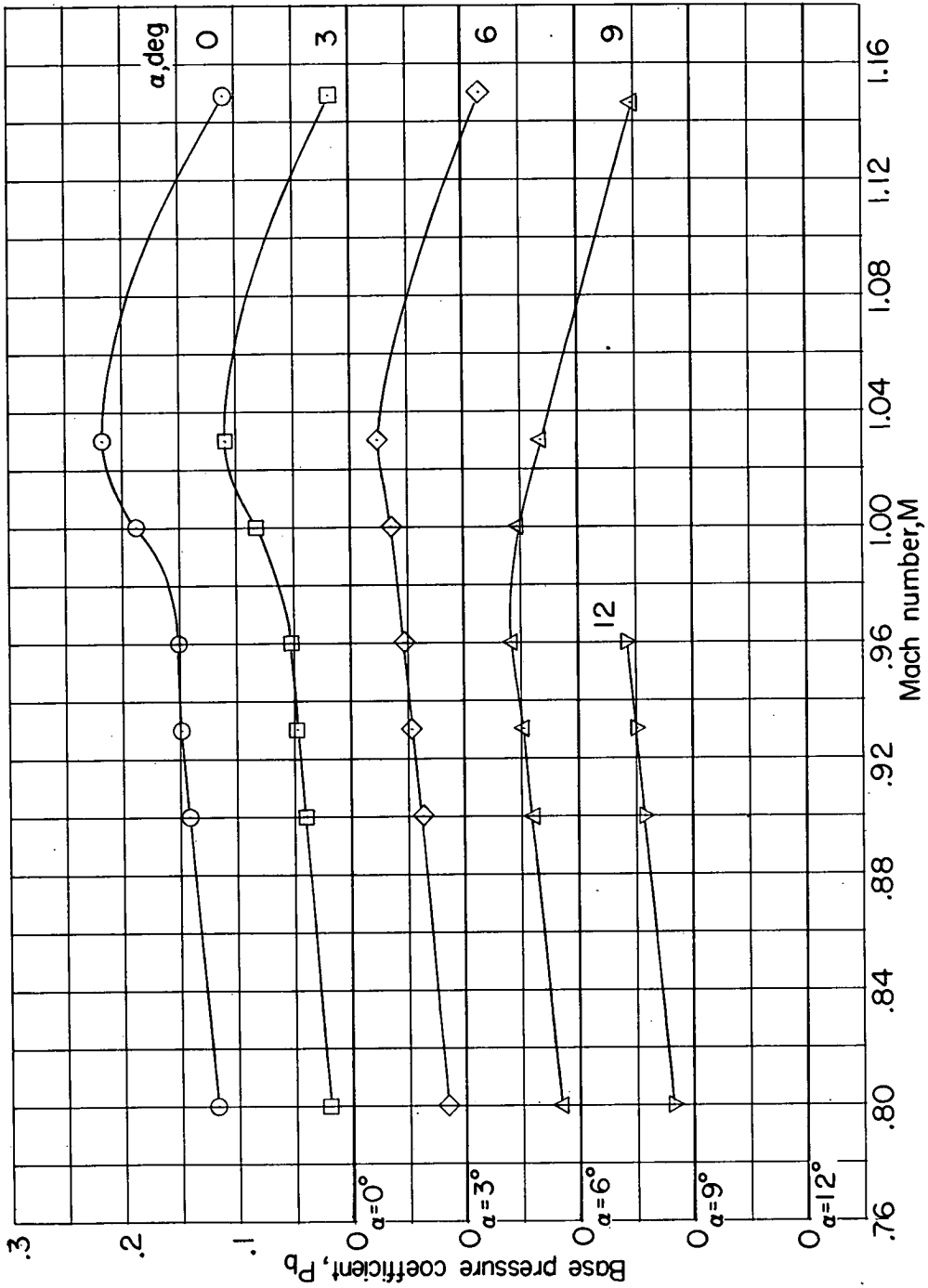
(a) Body with partial indentation.

Figure 4.- Variation with Mach number of base-pressure coefficient for wing-body combinations.



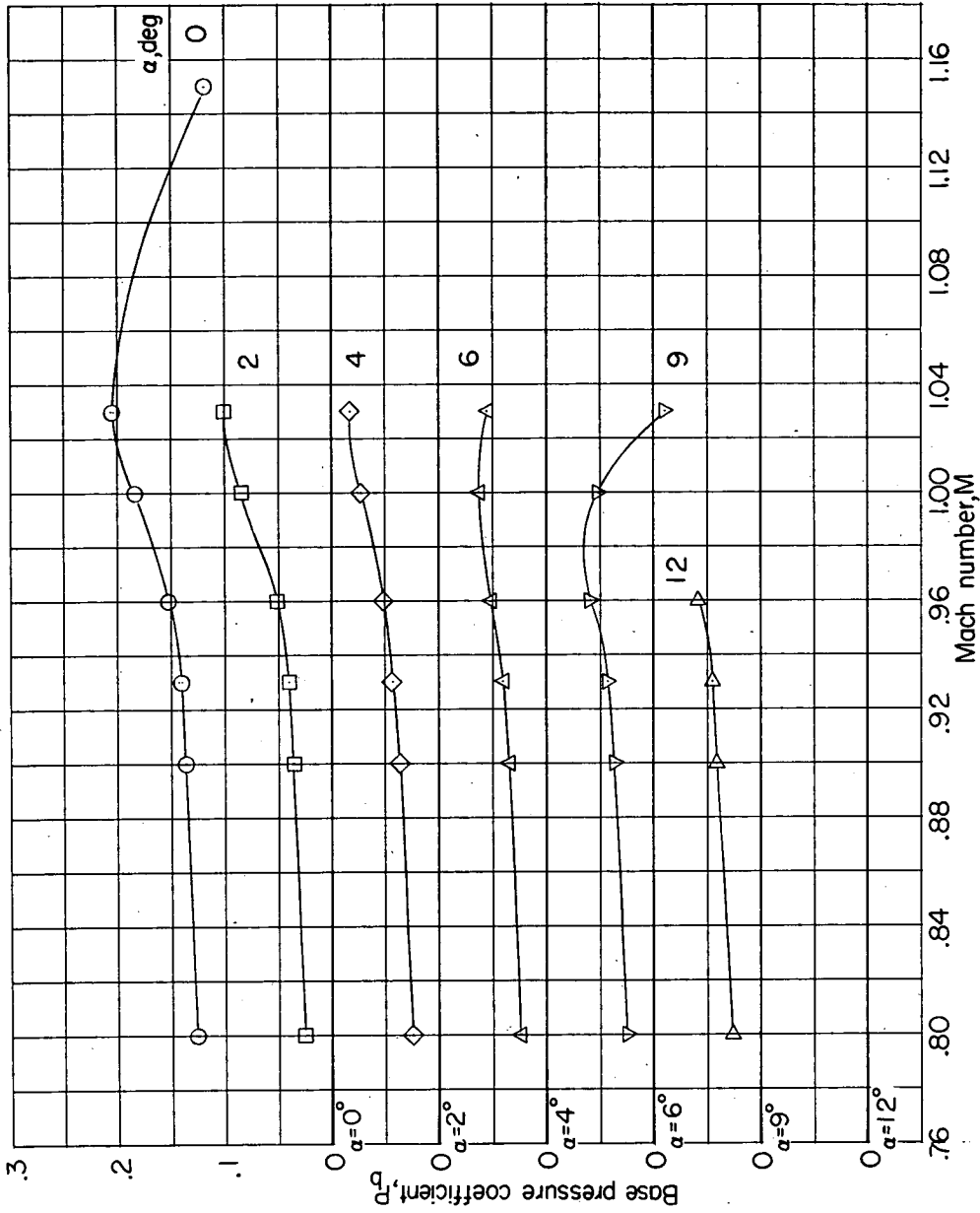
(b) Body with side indentation.

Figure 4.- Continued.



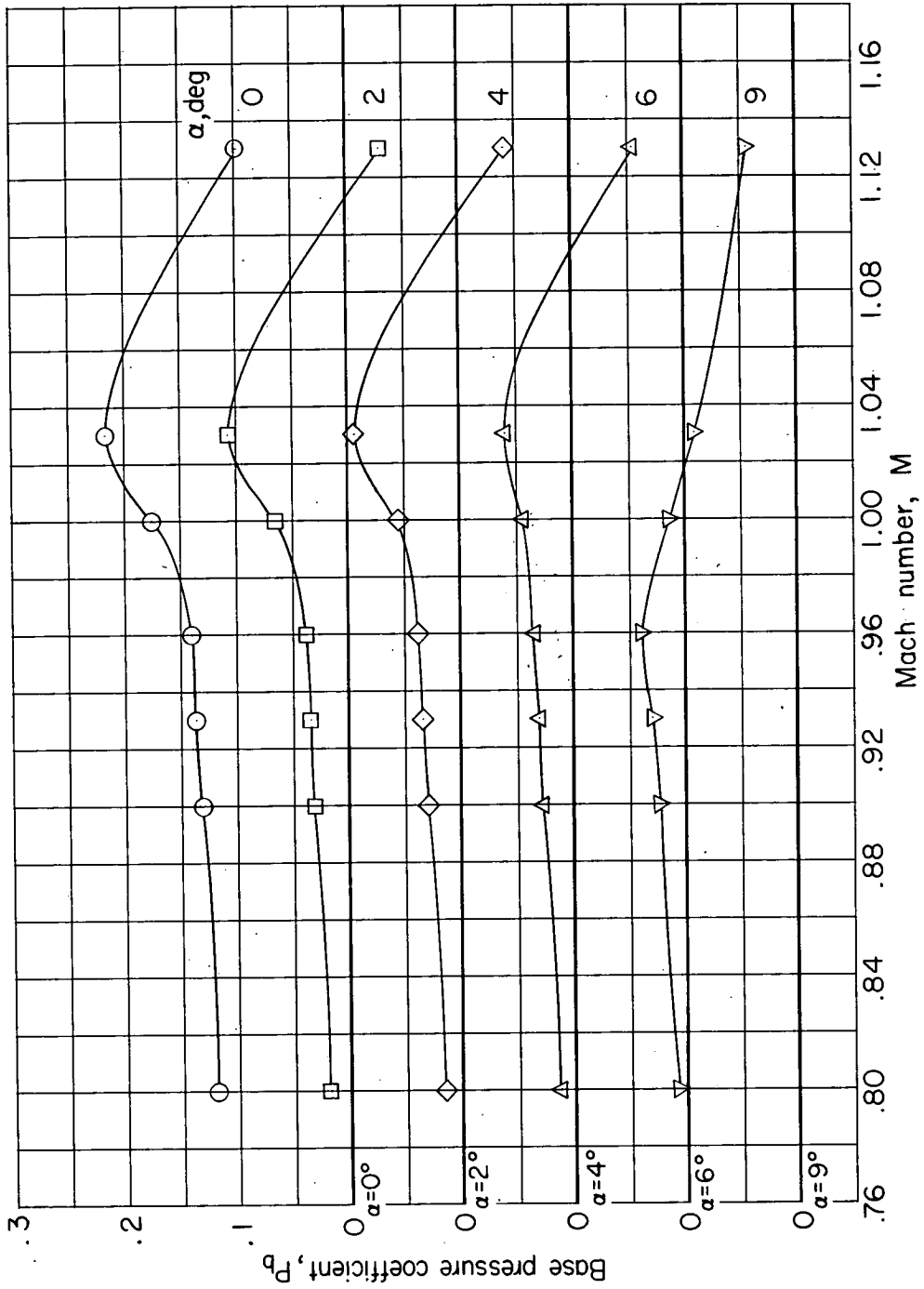
(c) Body with deep, rapid indentation.

Figure 4.- Continued.



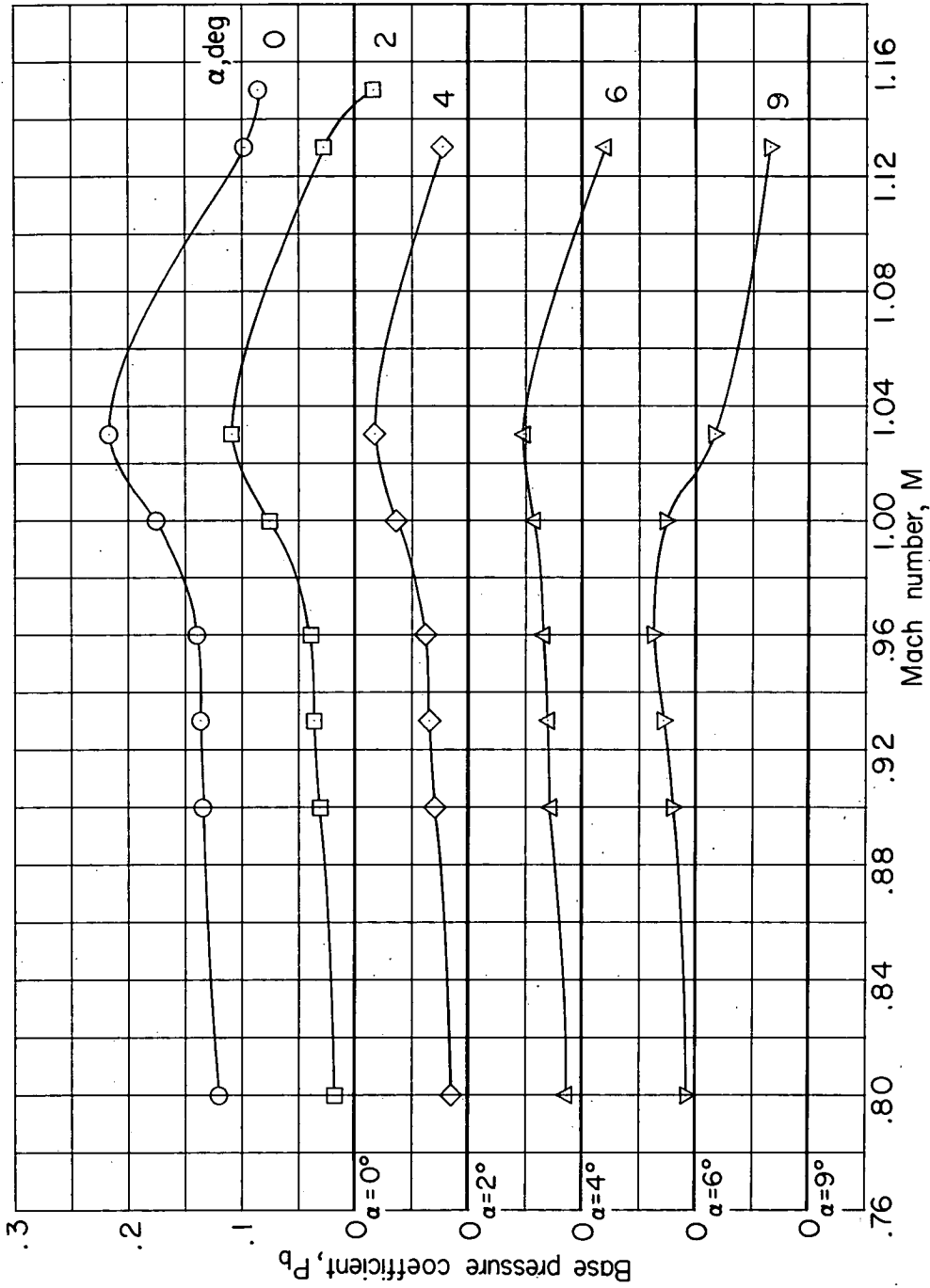
(d) Body with moderate, rapid indentation.

Figure 4.- Continued.



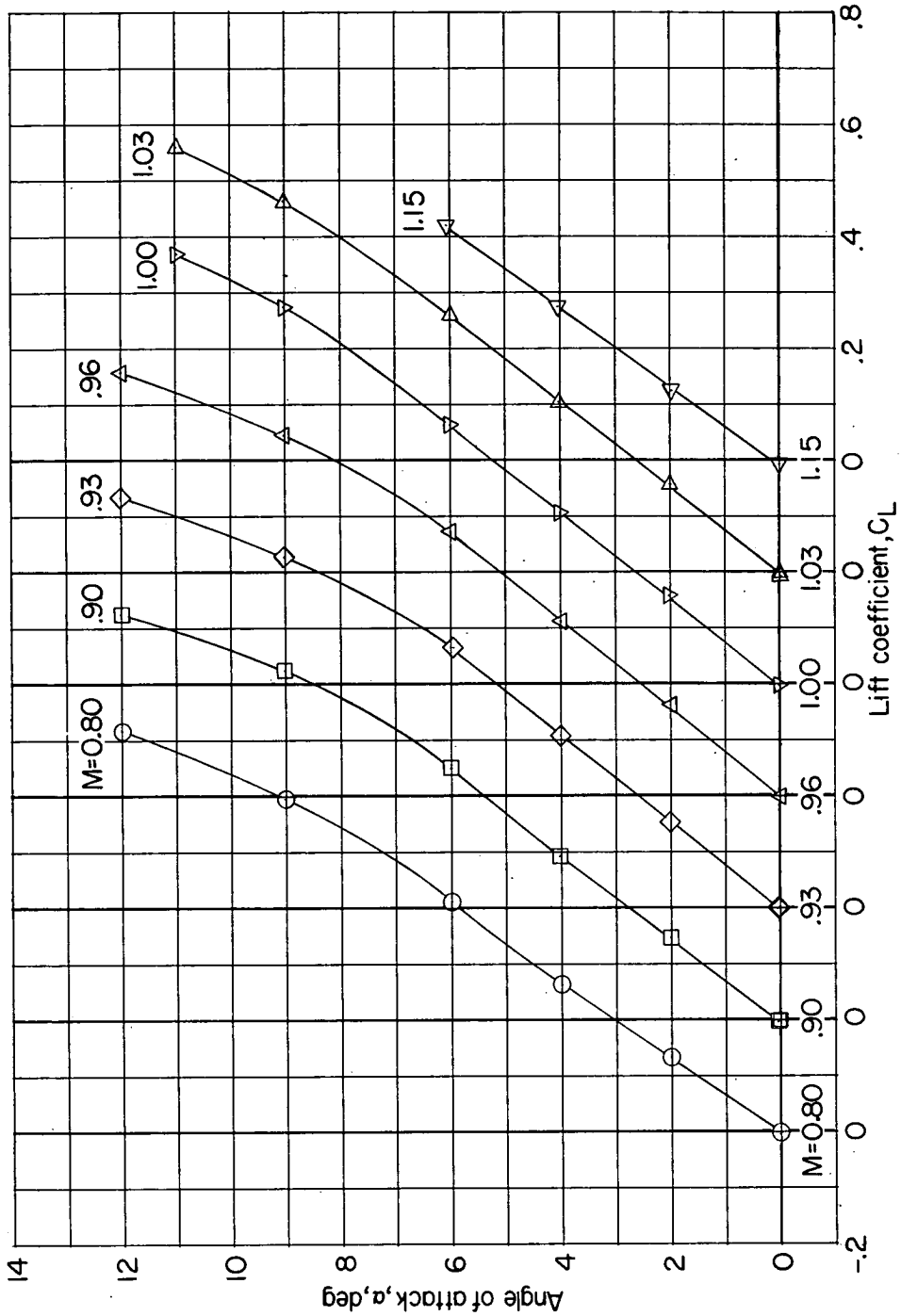
(e) Body with upper, rapid indentation.

Figure 4.- Continued.



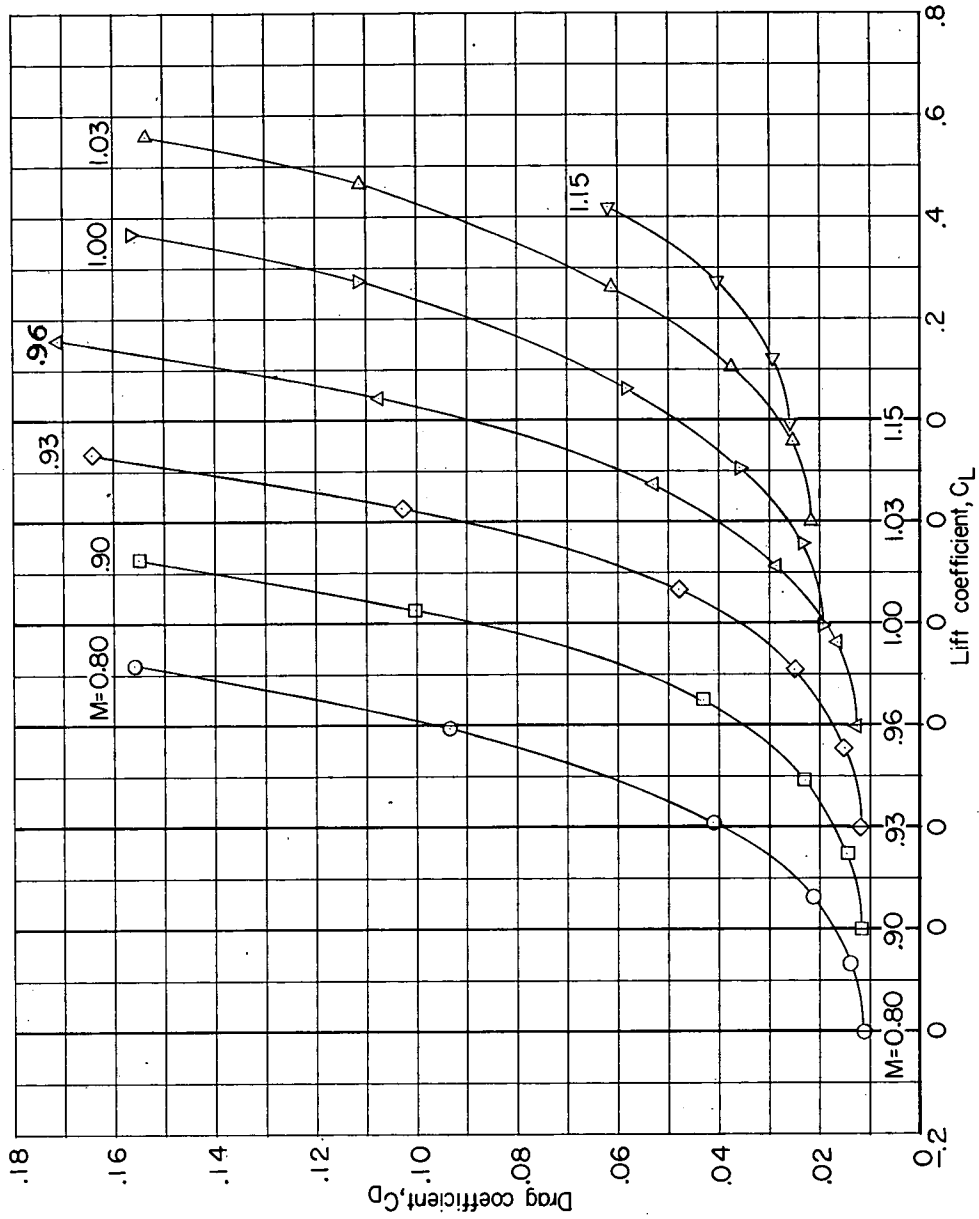
(f) Body with lower, rapid indentation.

Figure 4.- Concluded.



(a) Angle of attack.

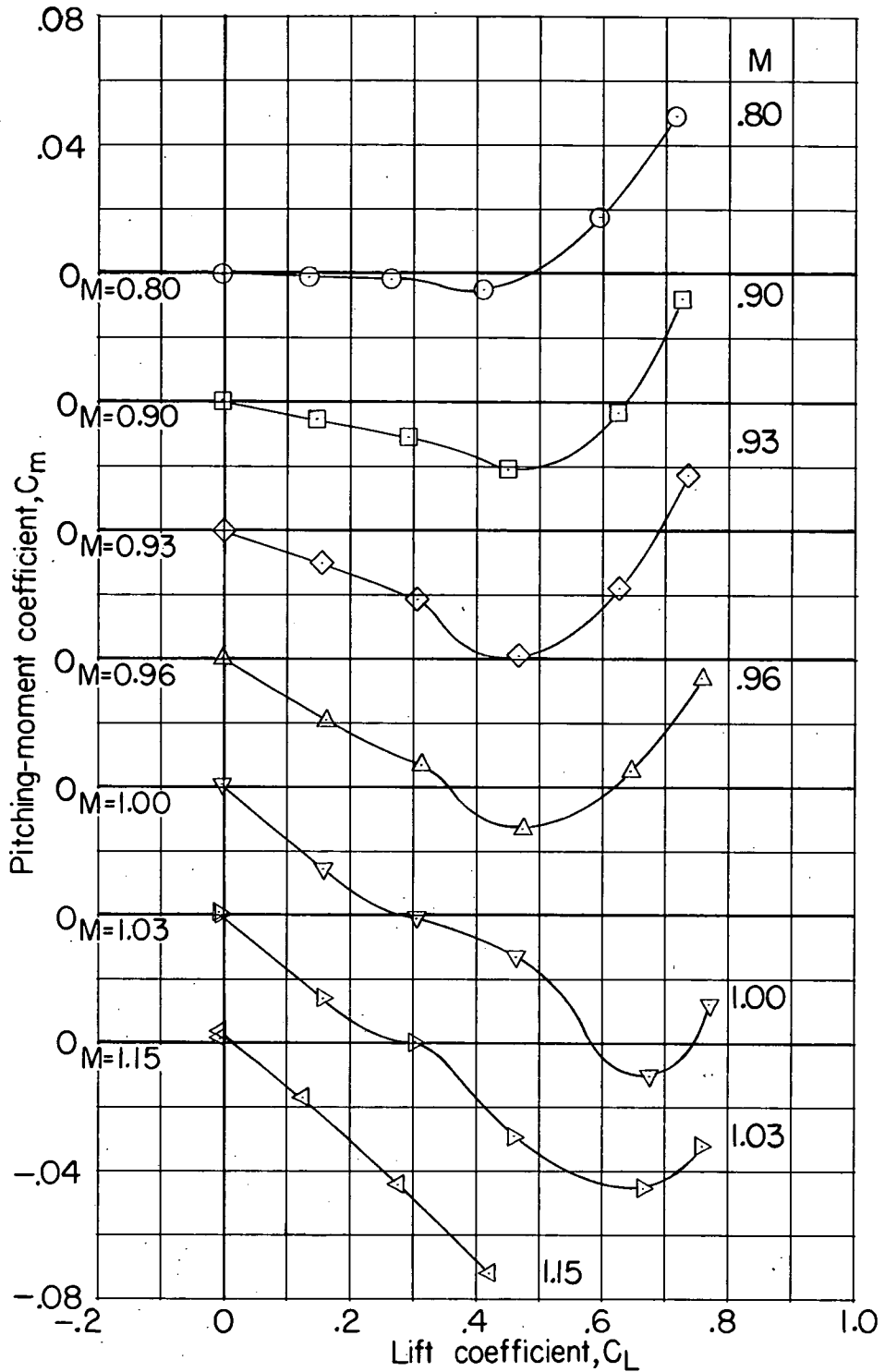
Figure 5.- Aerodynamic characteristics of partially indented wing-body combination.



(b) Drag coefficient.

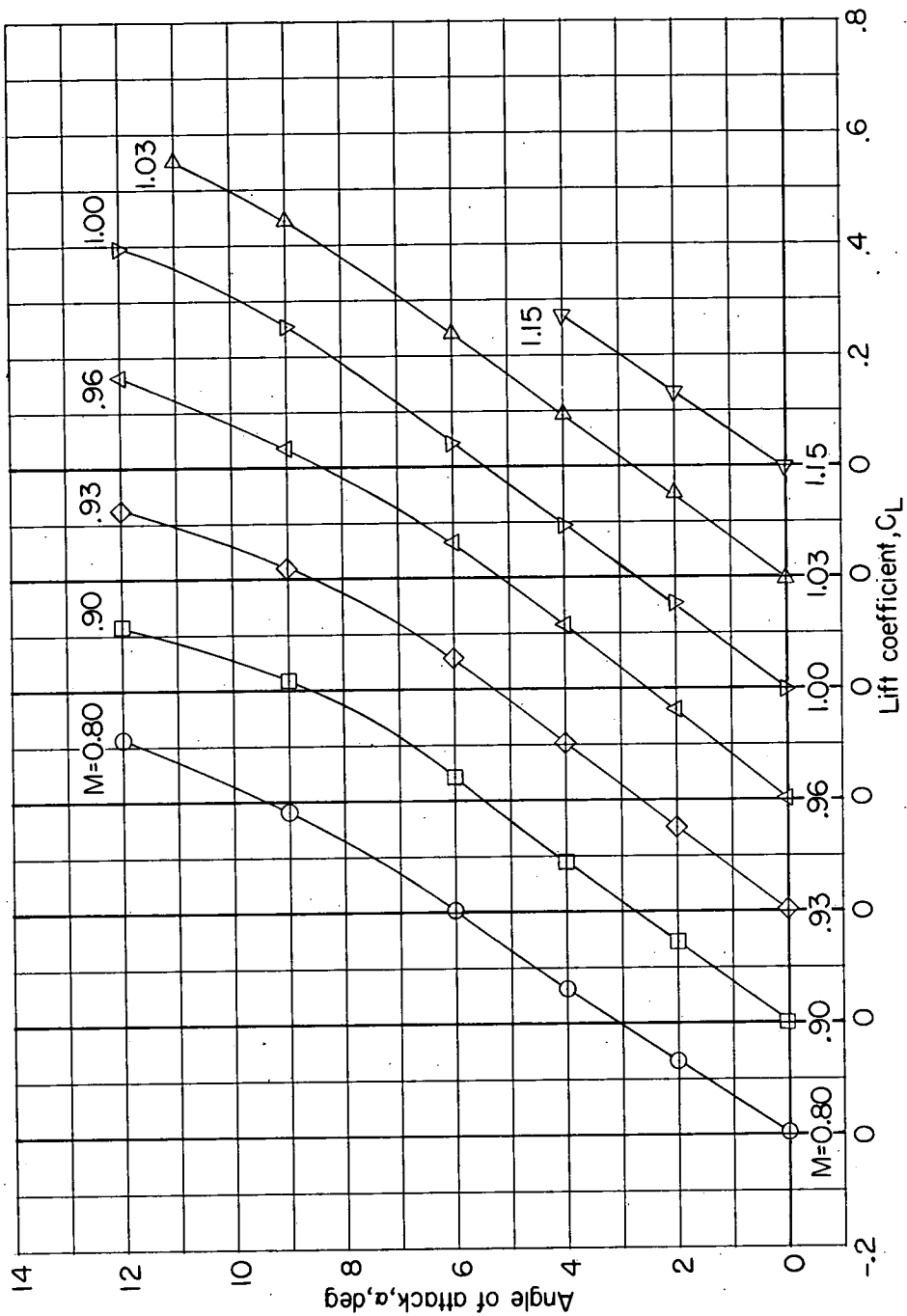
Figure 5.- Continued.





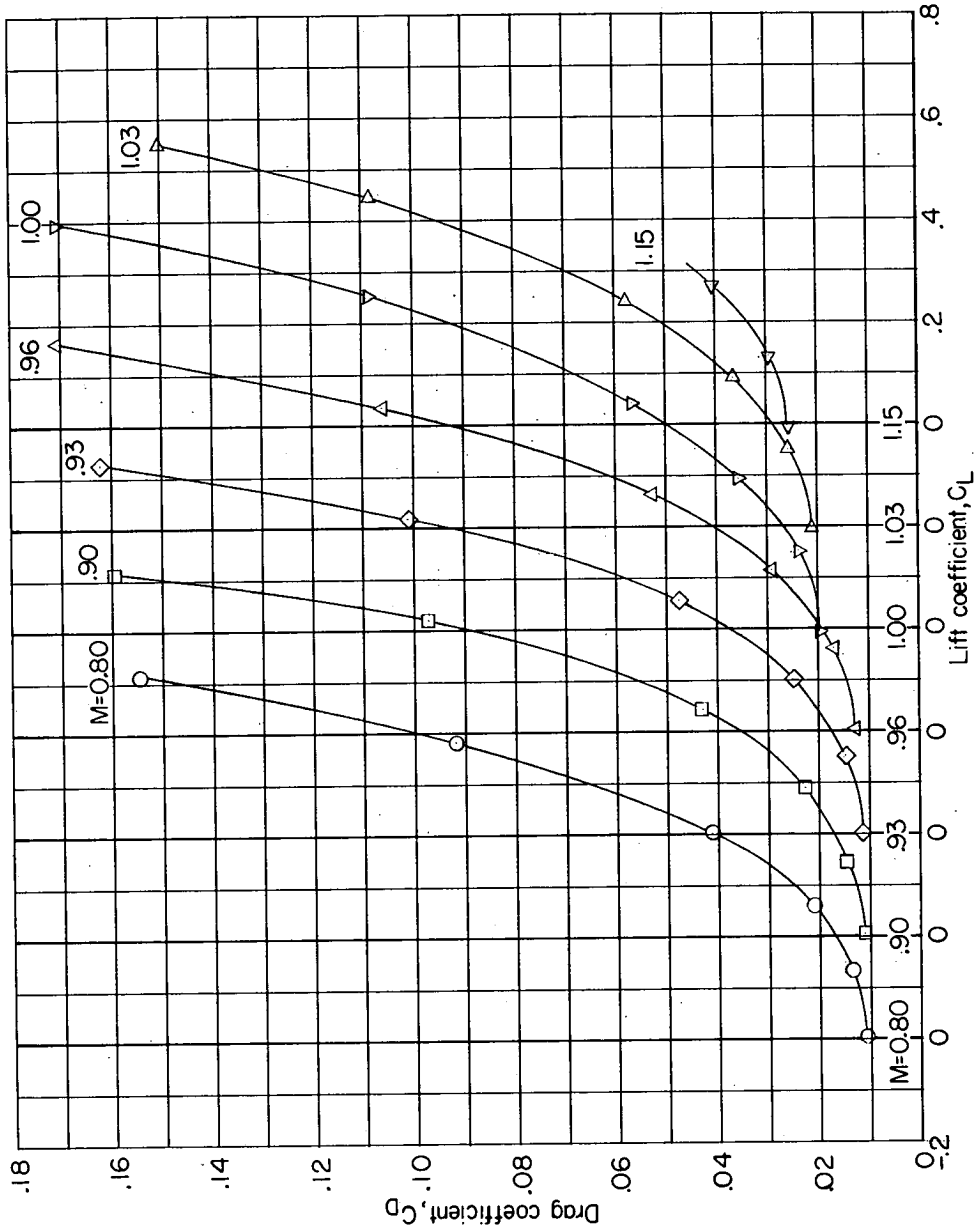
(c) Pitching-moment coefficient.

Figure 5.- Concluded.



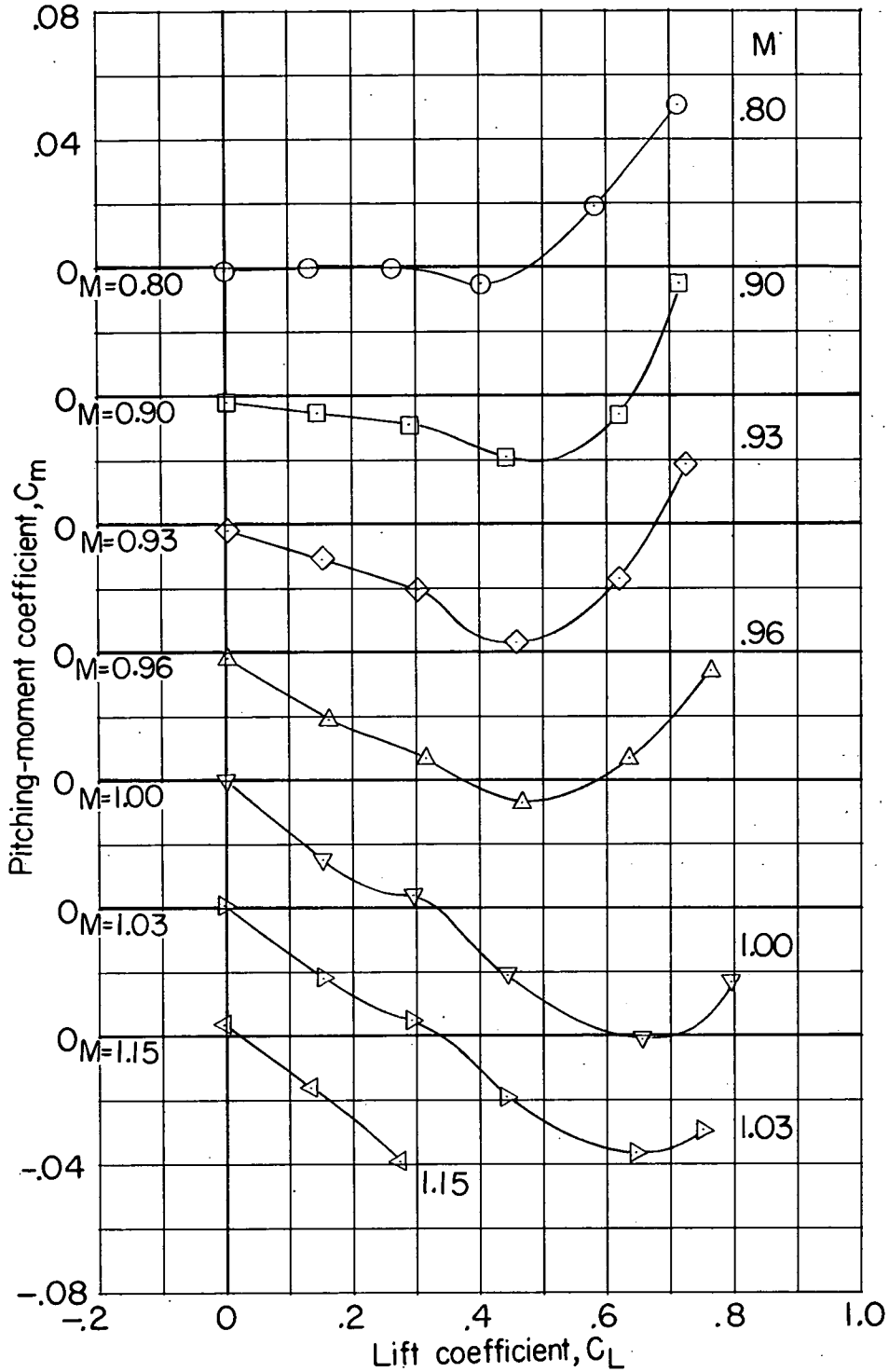
(a) Angle of attack.

Figure 6.- Aerodynamic characteristics of wing-body combination with side indentation.



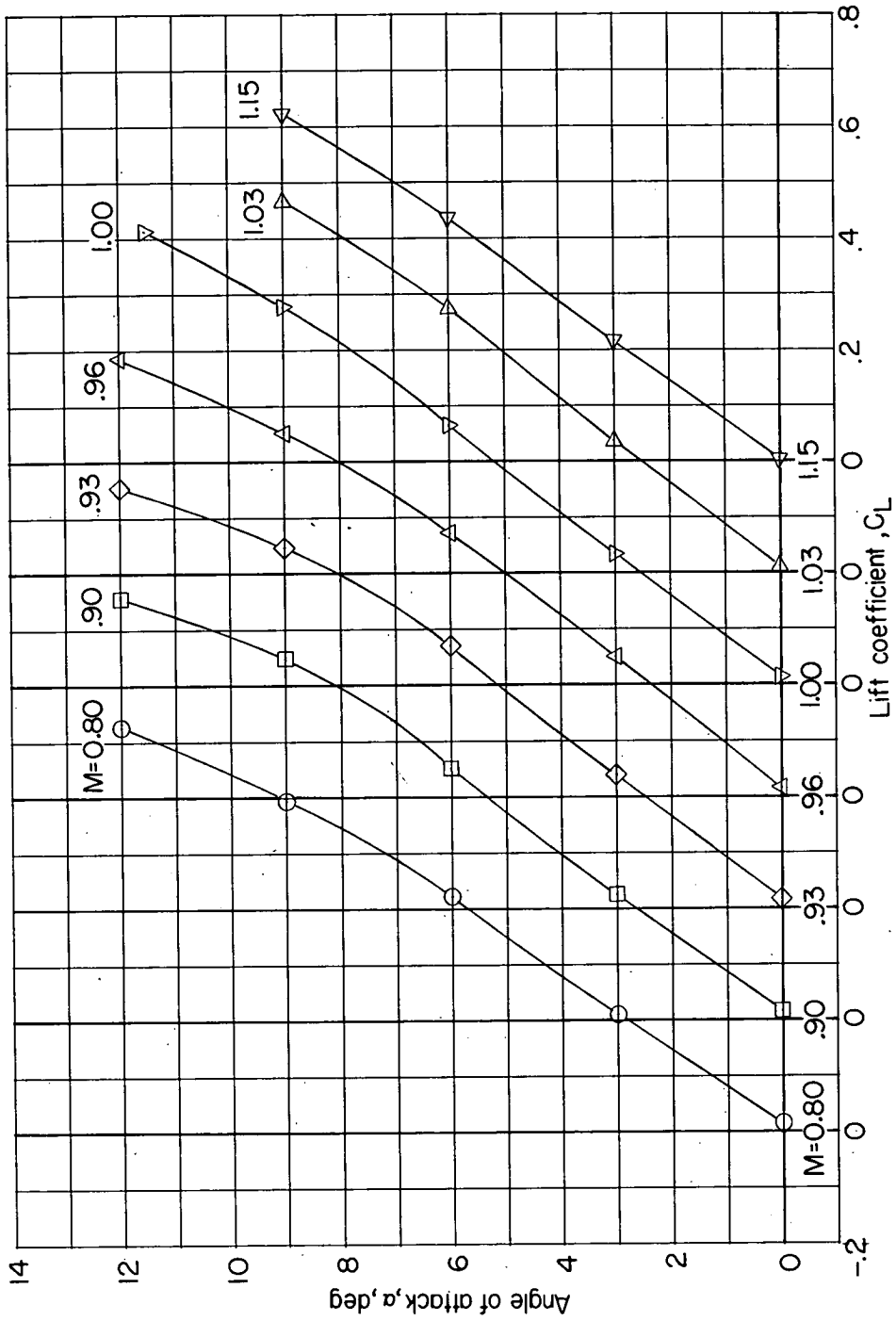
(b) Drag coefficient.

Figure 6.- Continued.



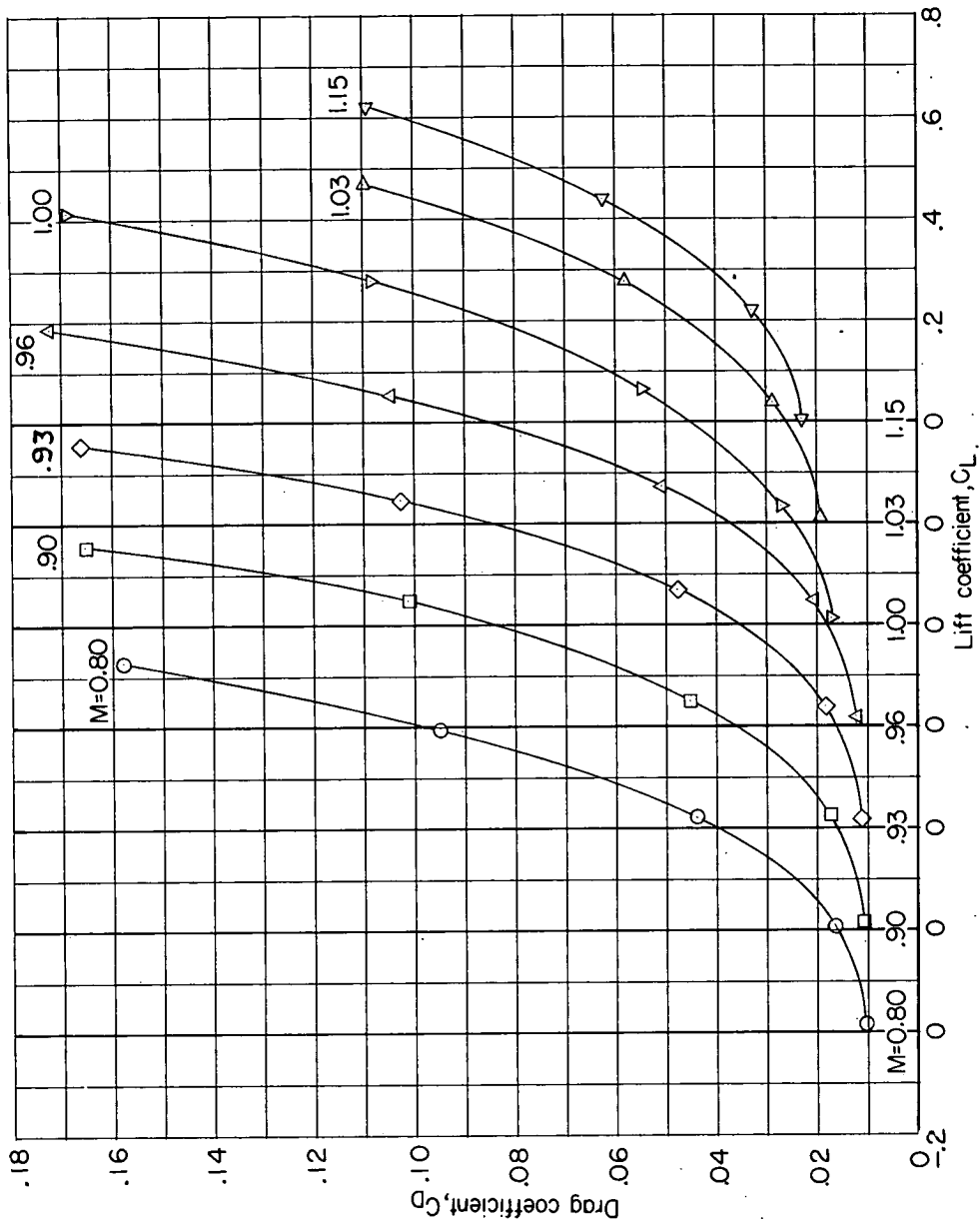
(c) Pitching-moment coefficient.

Figure 6.- Concluded.



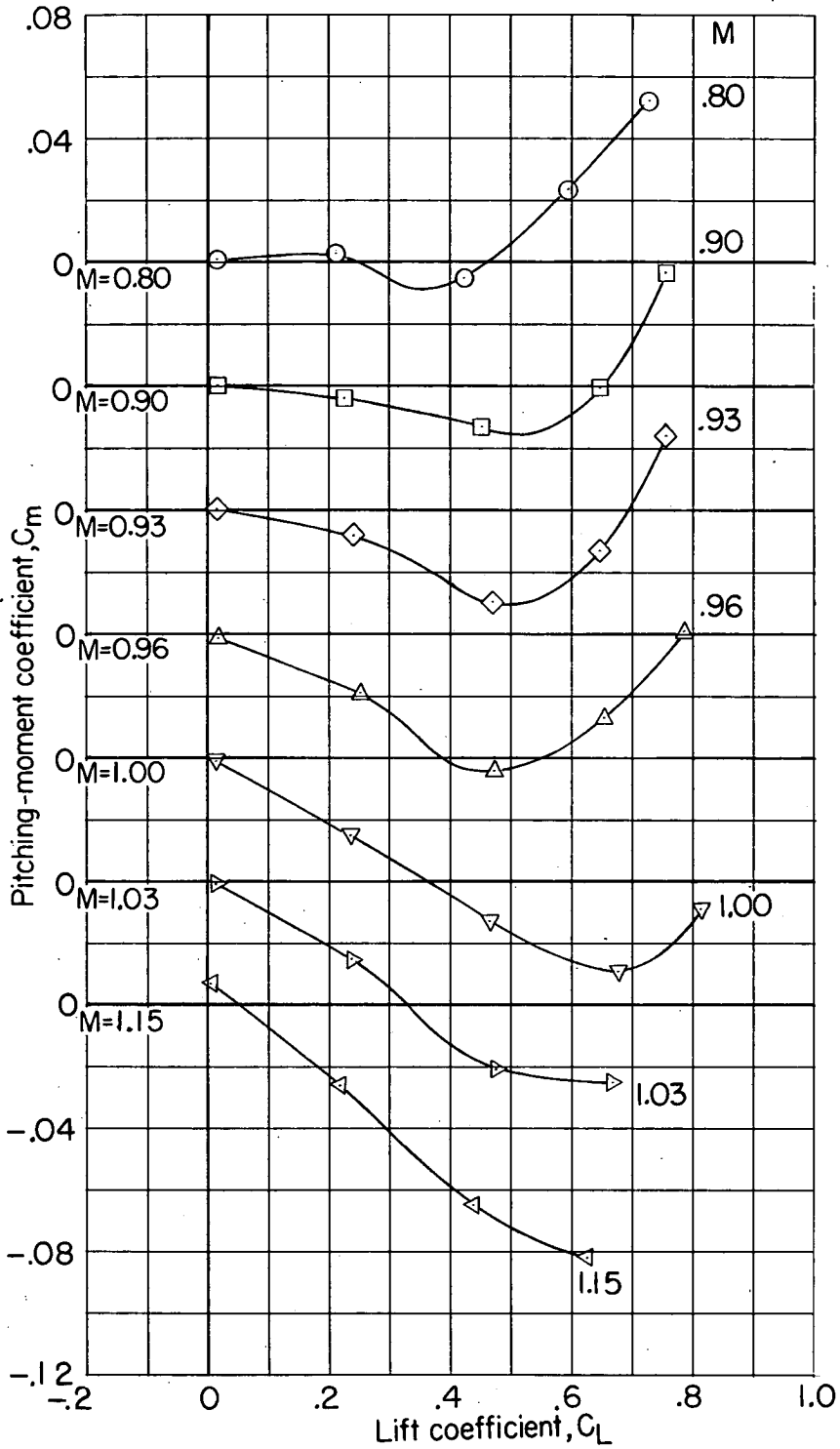
(a) Angle of attack.

Figure 7.- Aerodynamic characteristics of wing-body combination with deep, rapid indentation.



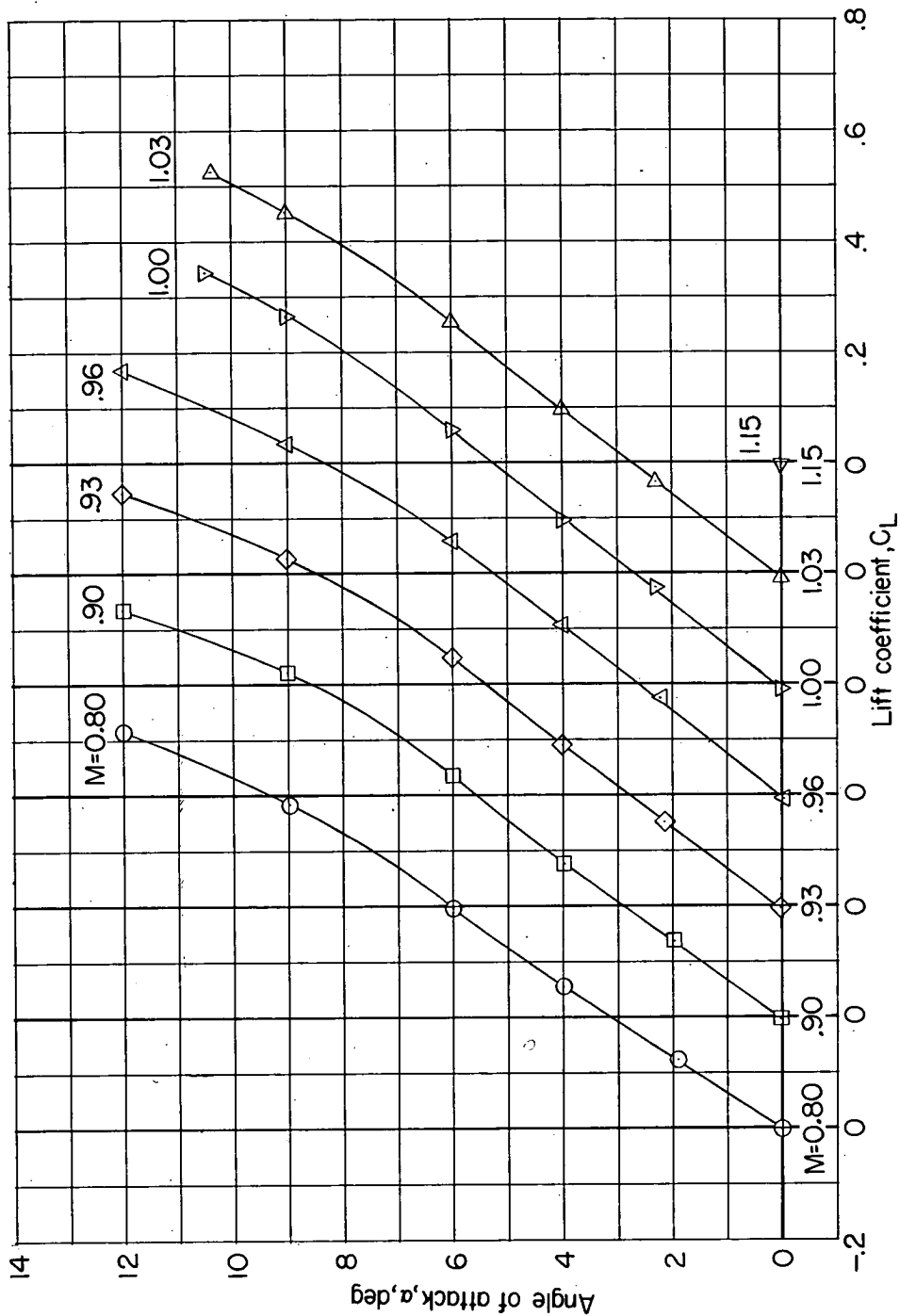
(b) Drag coefficient.

Figure 7.- Continued.



(c) Pitching-moment coefficient.

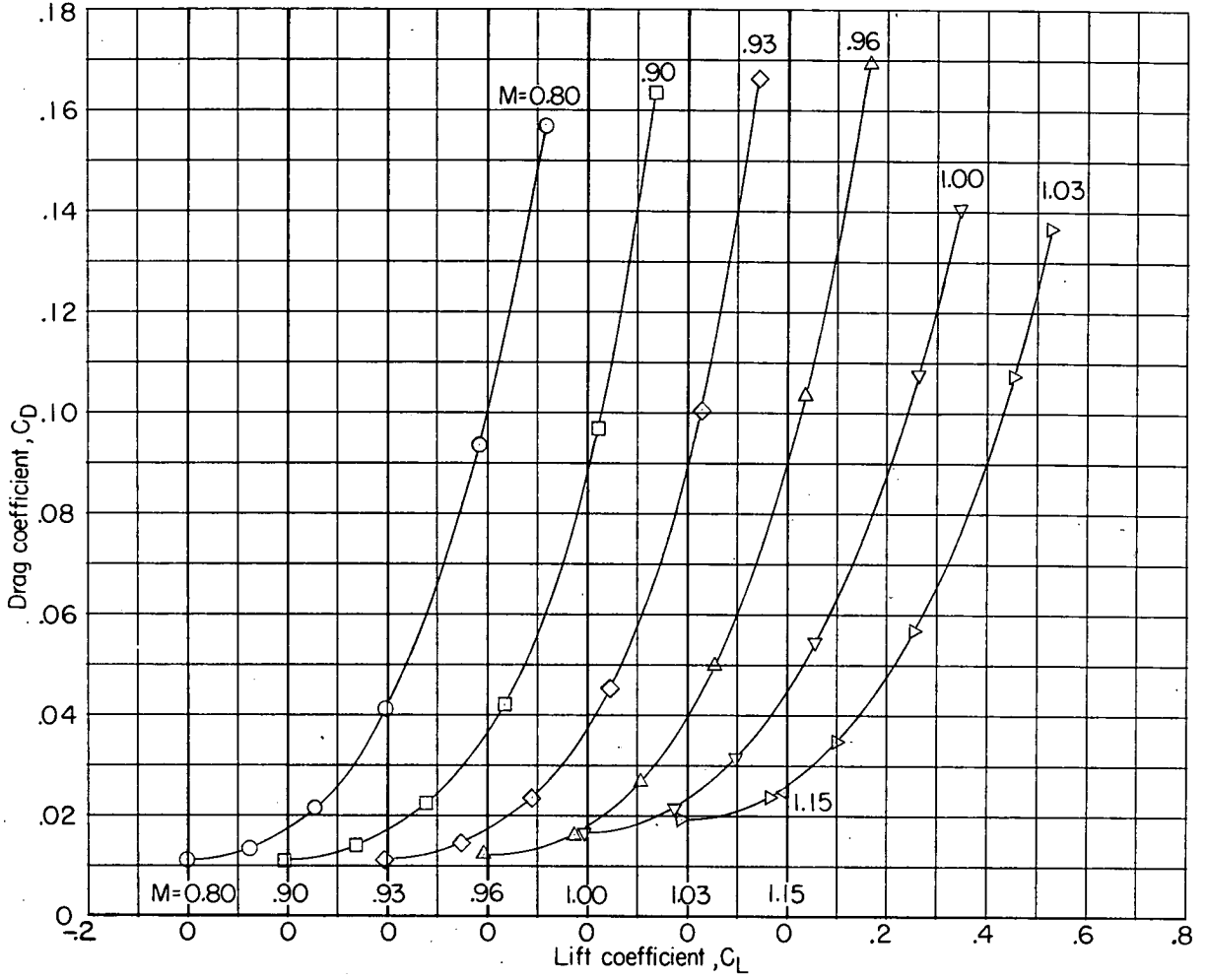
Figure 7.- Concluded.



(a) Angle of attack.

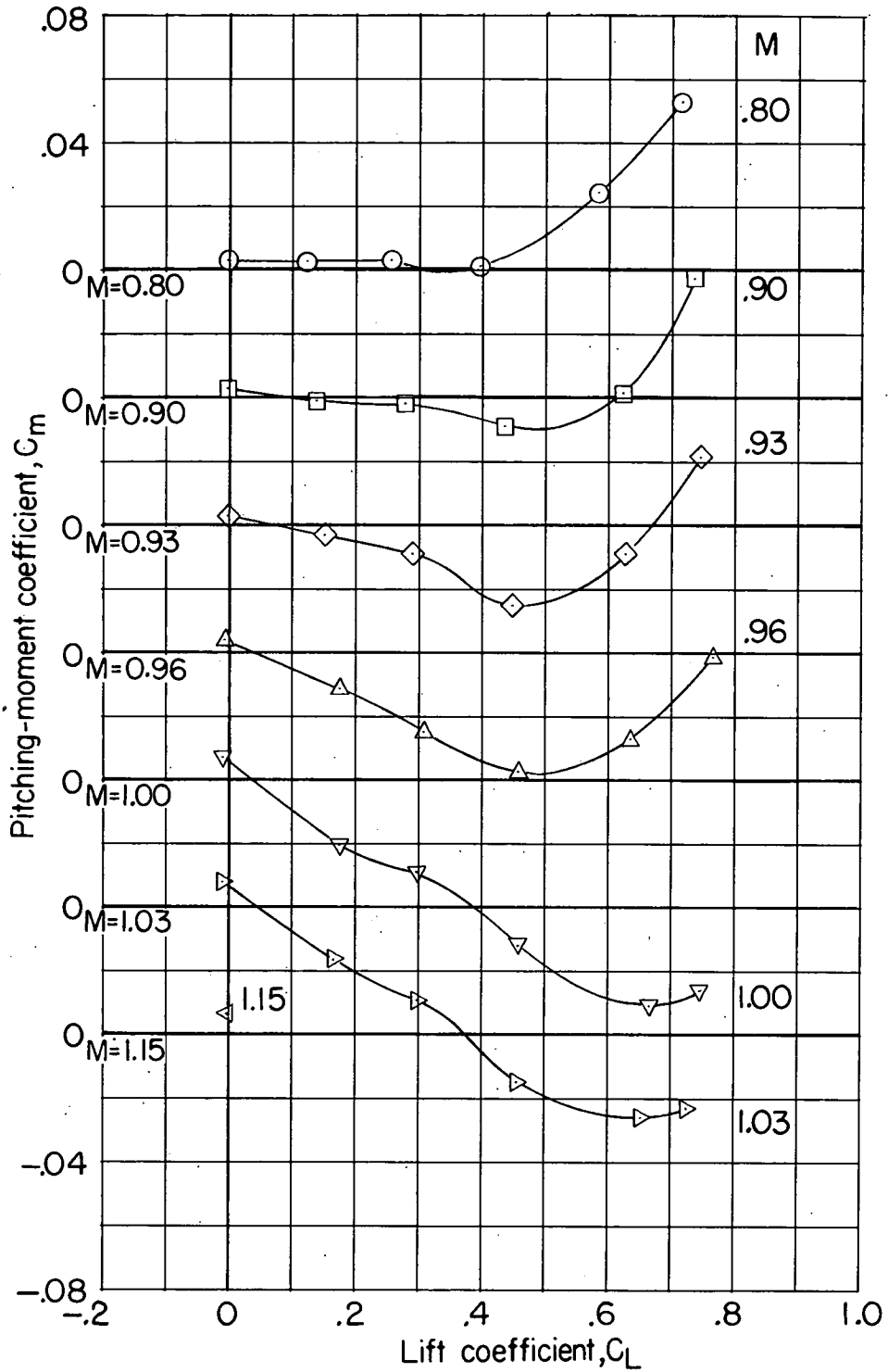
Figure 8.- Aerodynamic characteristics of wing-body combination with moderate, rapid indentation.





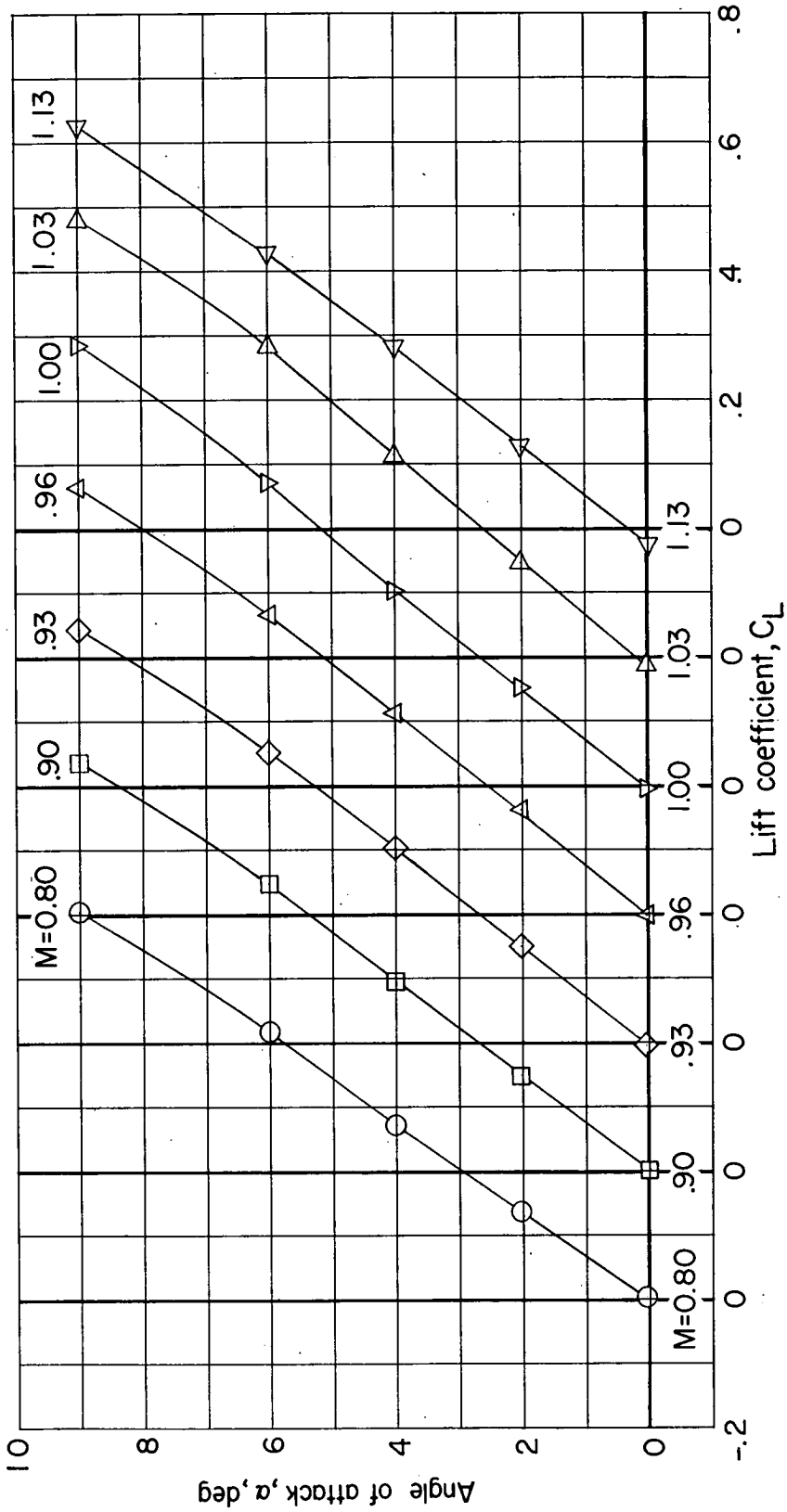
(b) Drag coefficient.

Figure 8.- Continued.



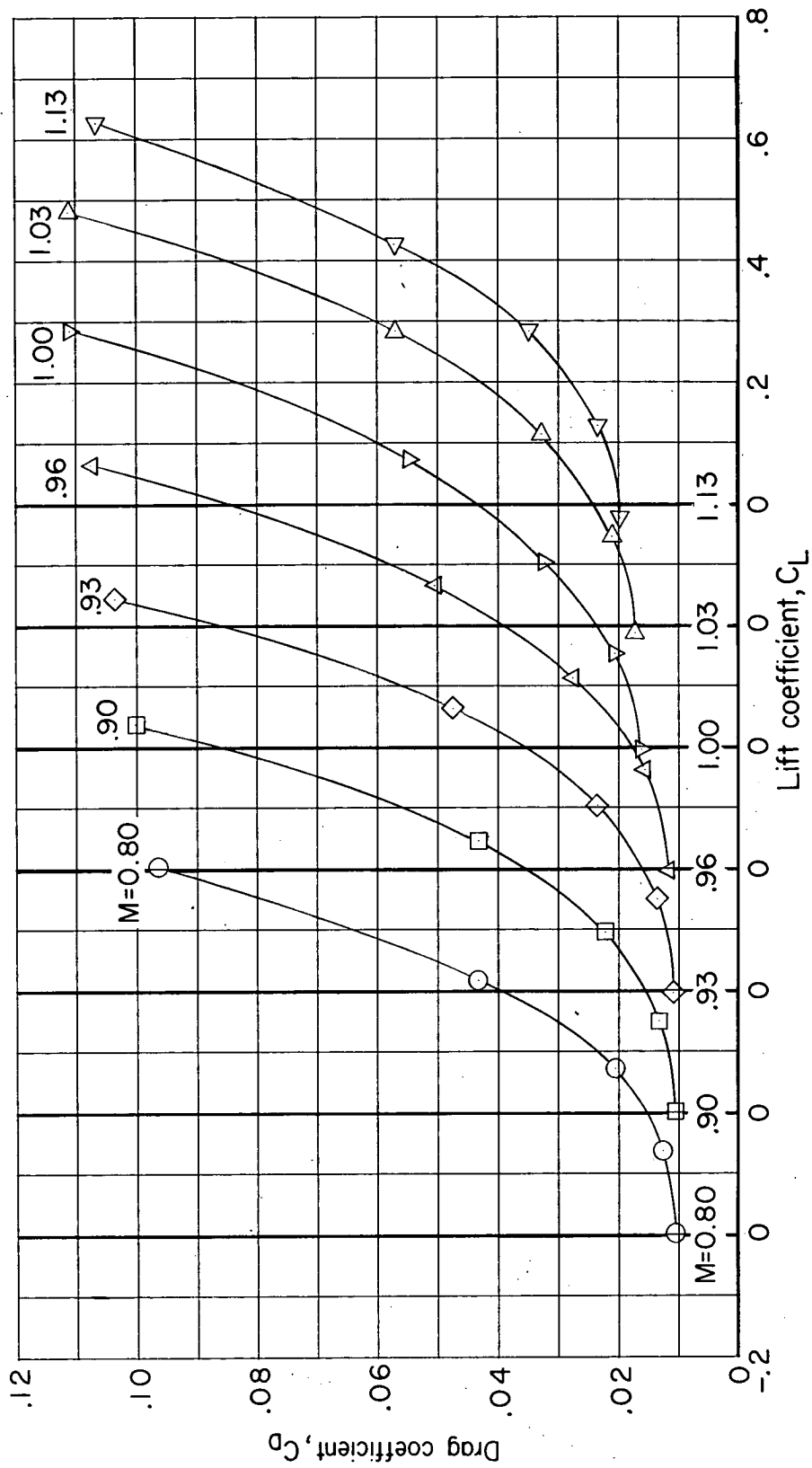
(c) Pitching-moment coefficient.

Figure 8.- Concluded.



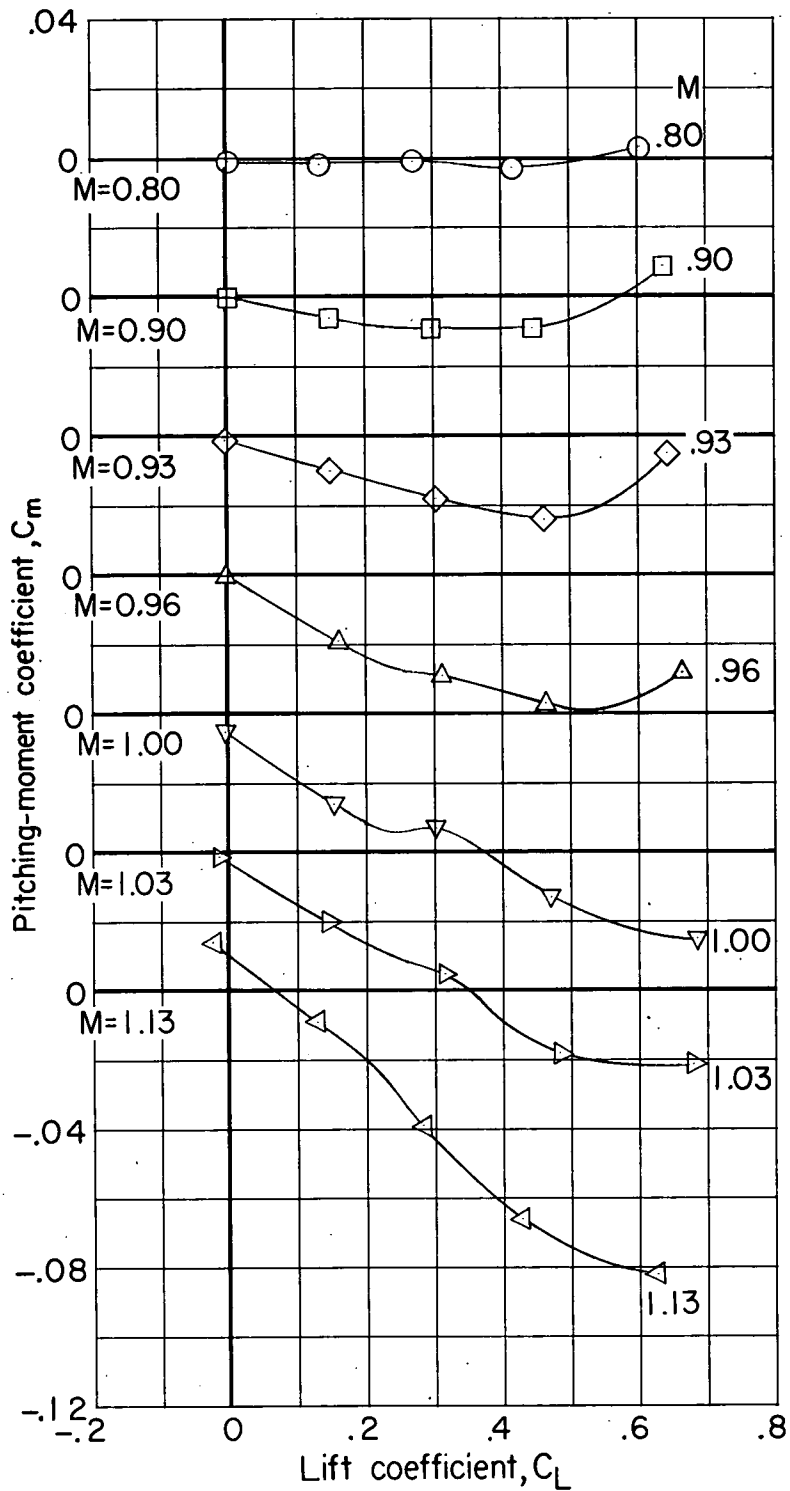
(a) Angle of attack.

Figure 9.- Aerodynamic characteristics of wing-body combination with upper, rapid indentation.



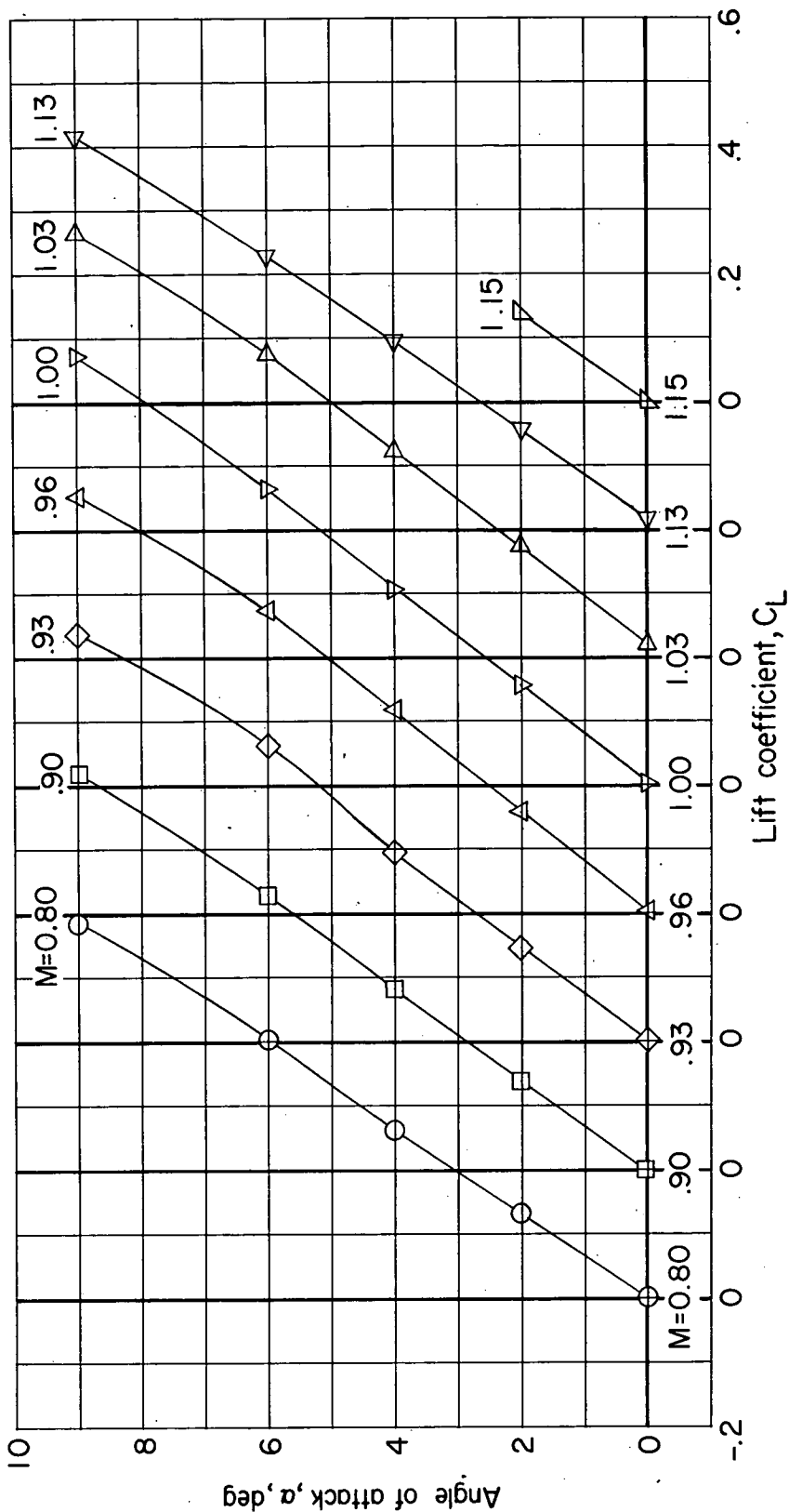
(b) Drag coefficient.

Figure 9.- Continued.



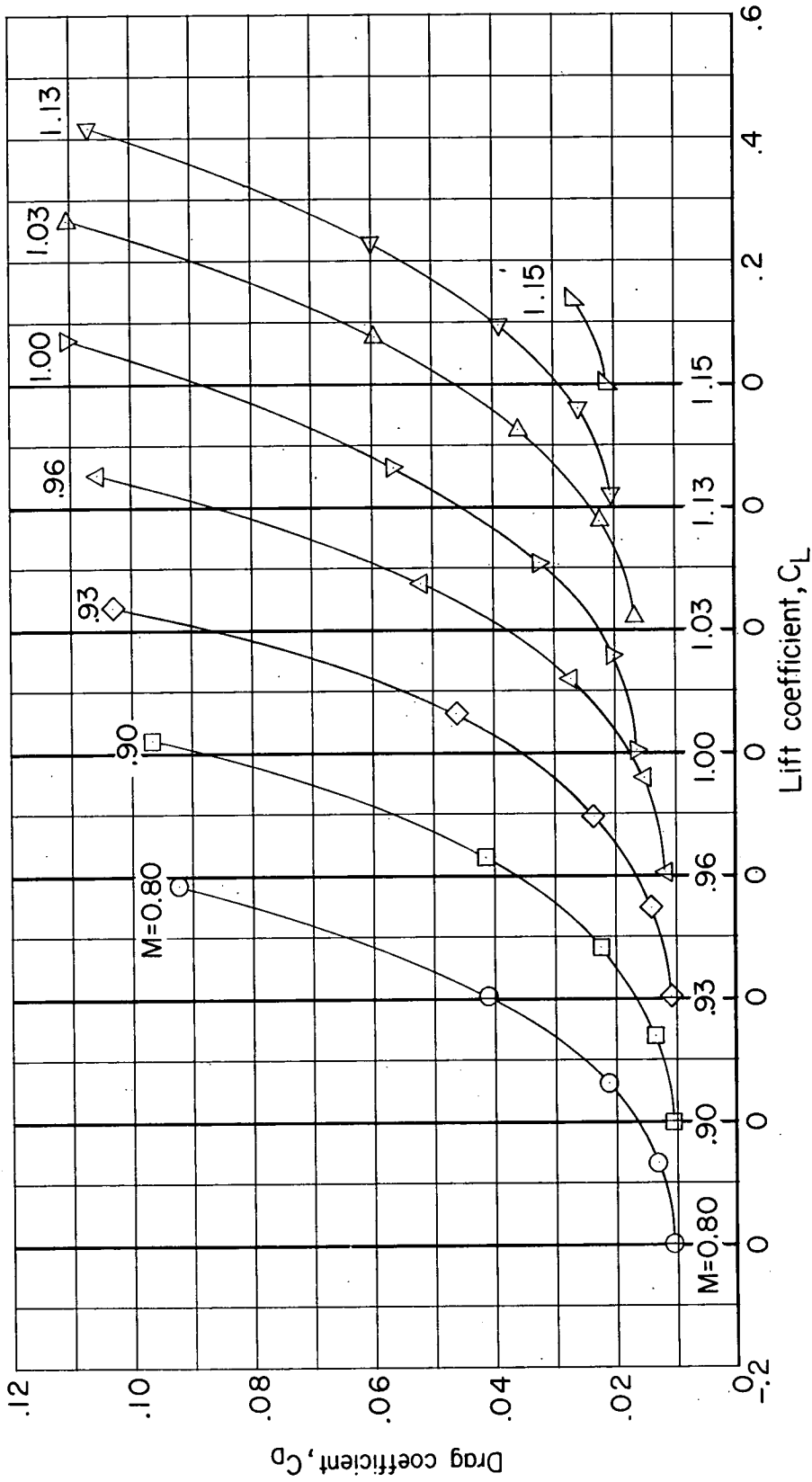
(c) Pitching-moment coefficient.

Figure 9.- Concluded.



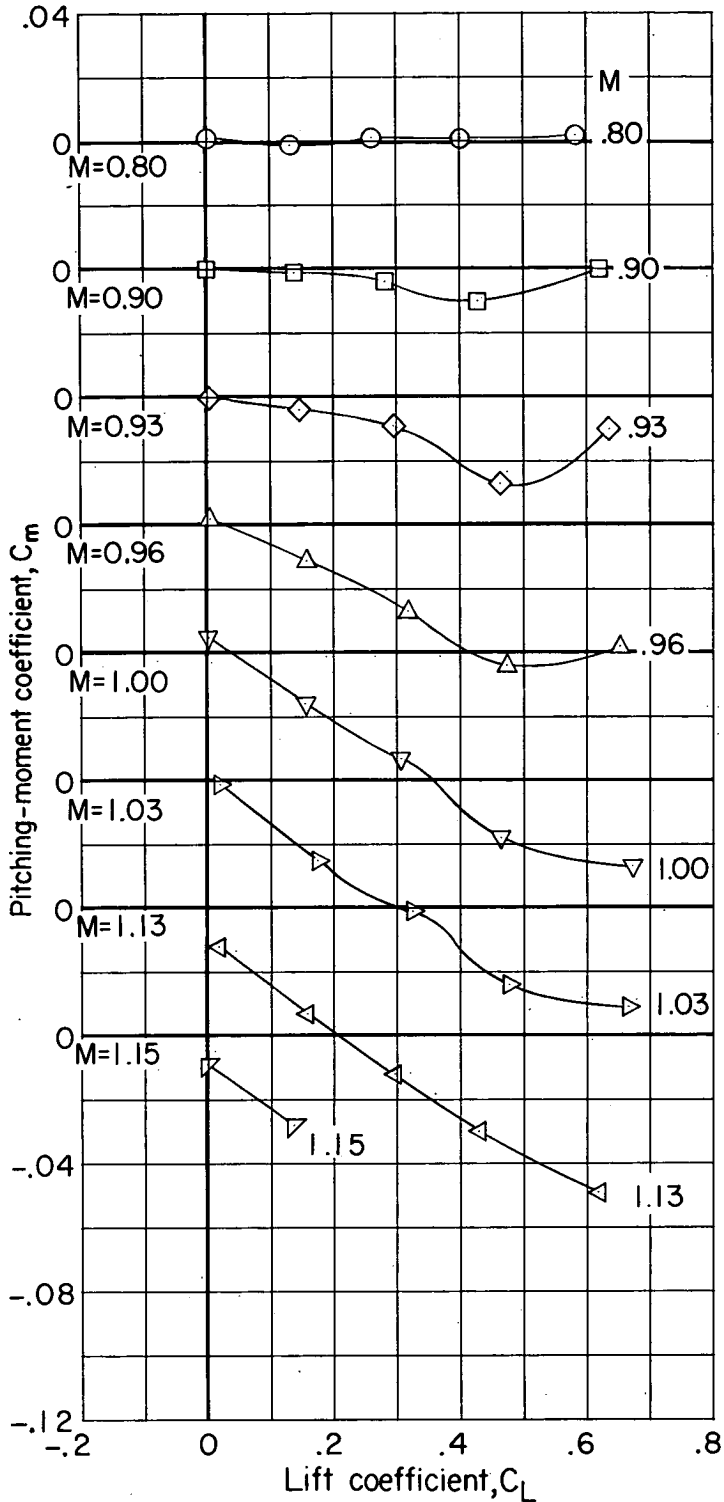
(a) Angle of attack.

Figure 10.- Aerodynamic characteristics of wing-body combination with lower, rapid indentation.



(b) Drag coefficient.

Figure 10.- Continued.



(c) Pitching-moment coefficient.

Figure 10.- Concluded.



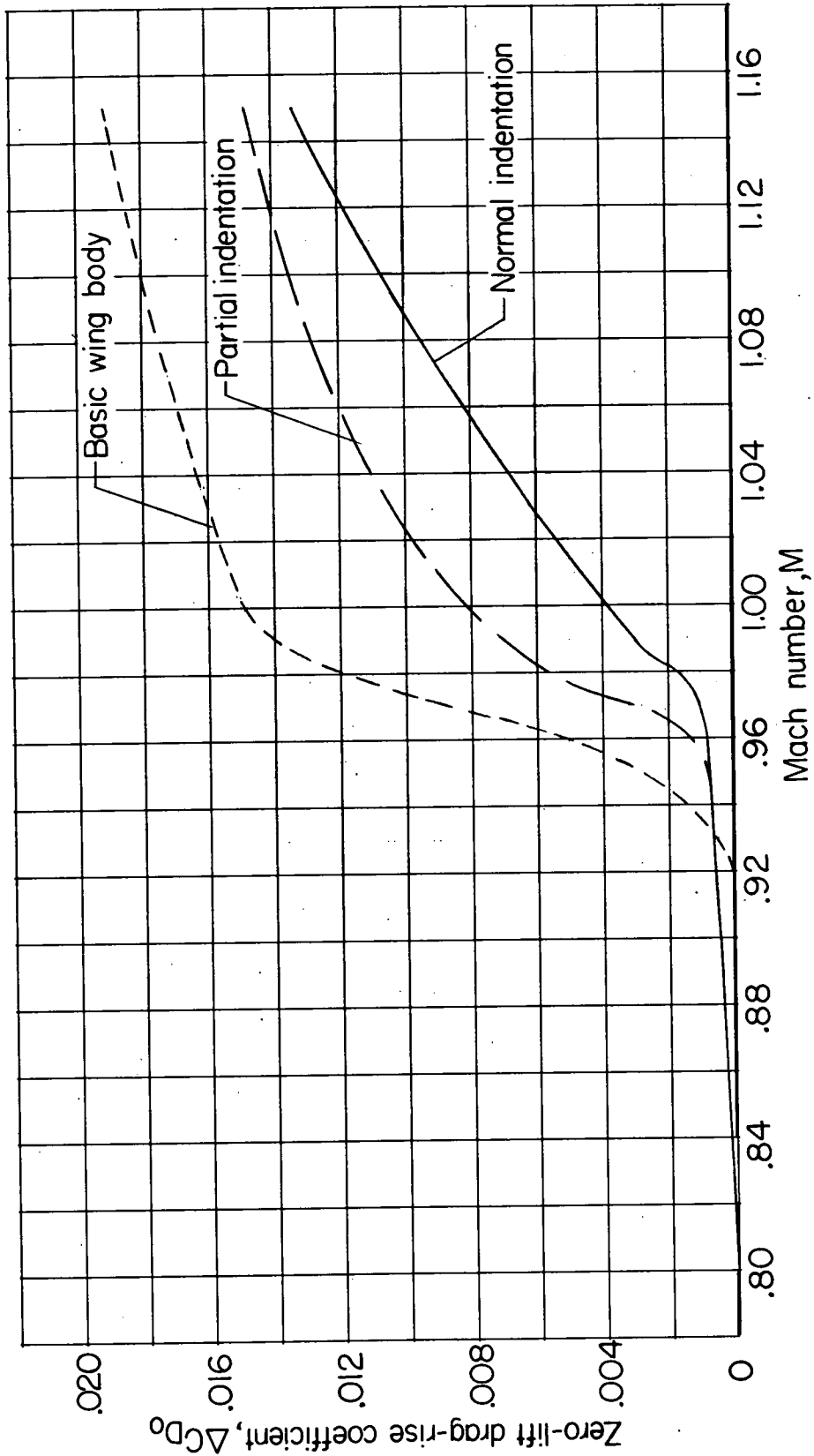


Figure 11.- Effect of partial indentation on the variation of zero-lift drag-rise coefficient with Mach number.

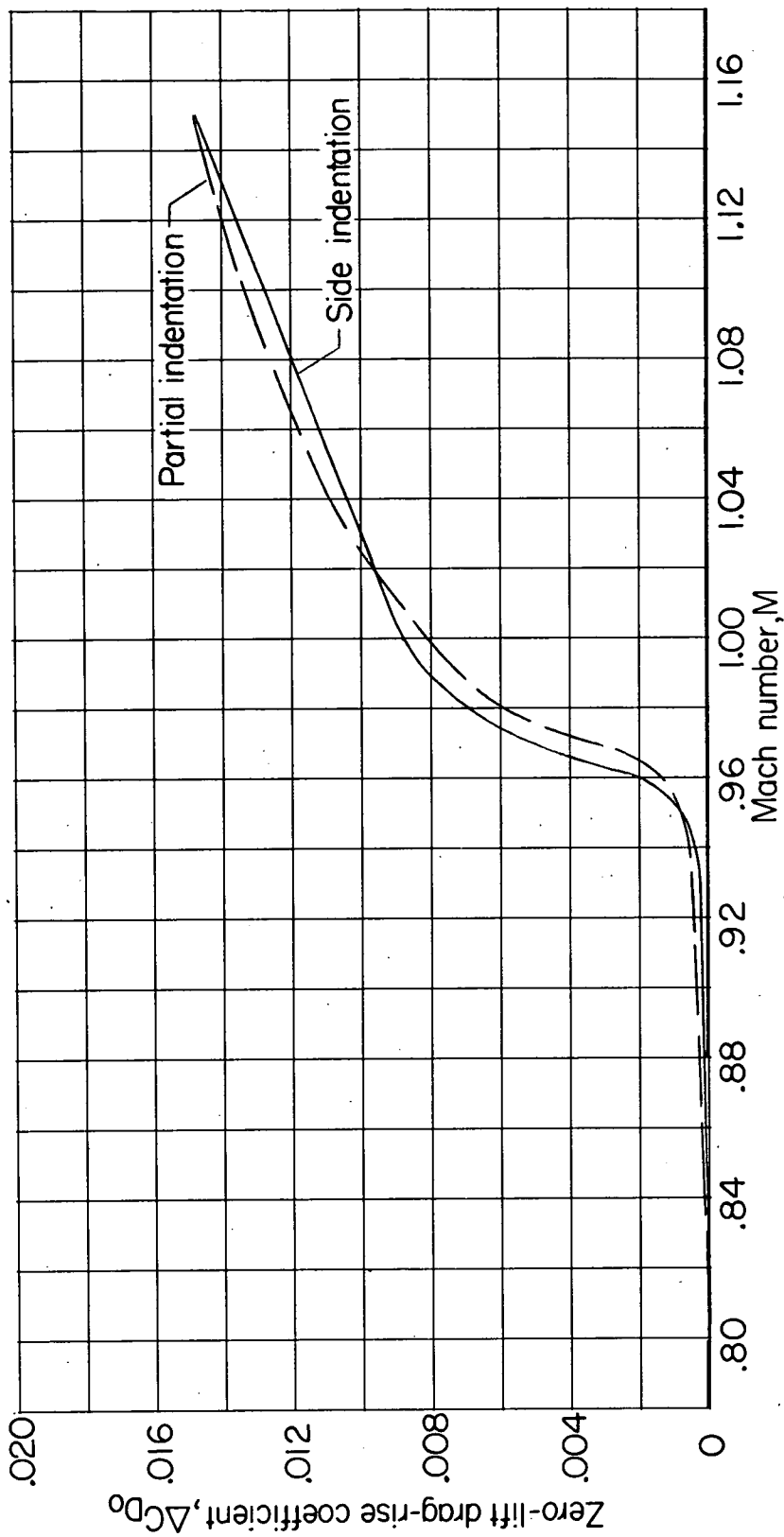


Figure 12.- Effect of side indentation on the variation of zero-lift drag-rise coefficient with Mach number.

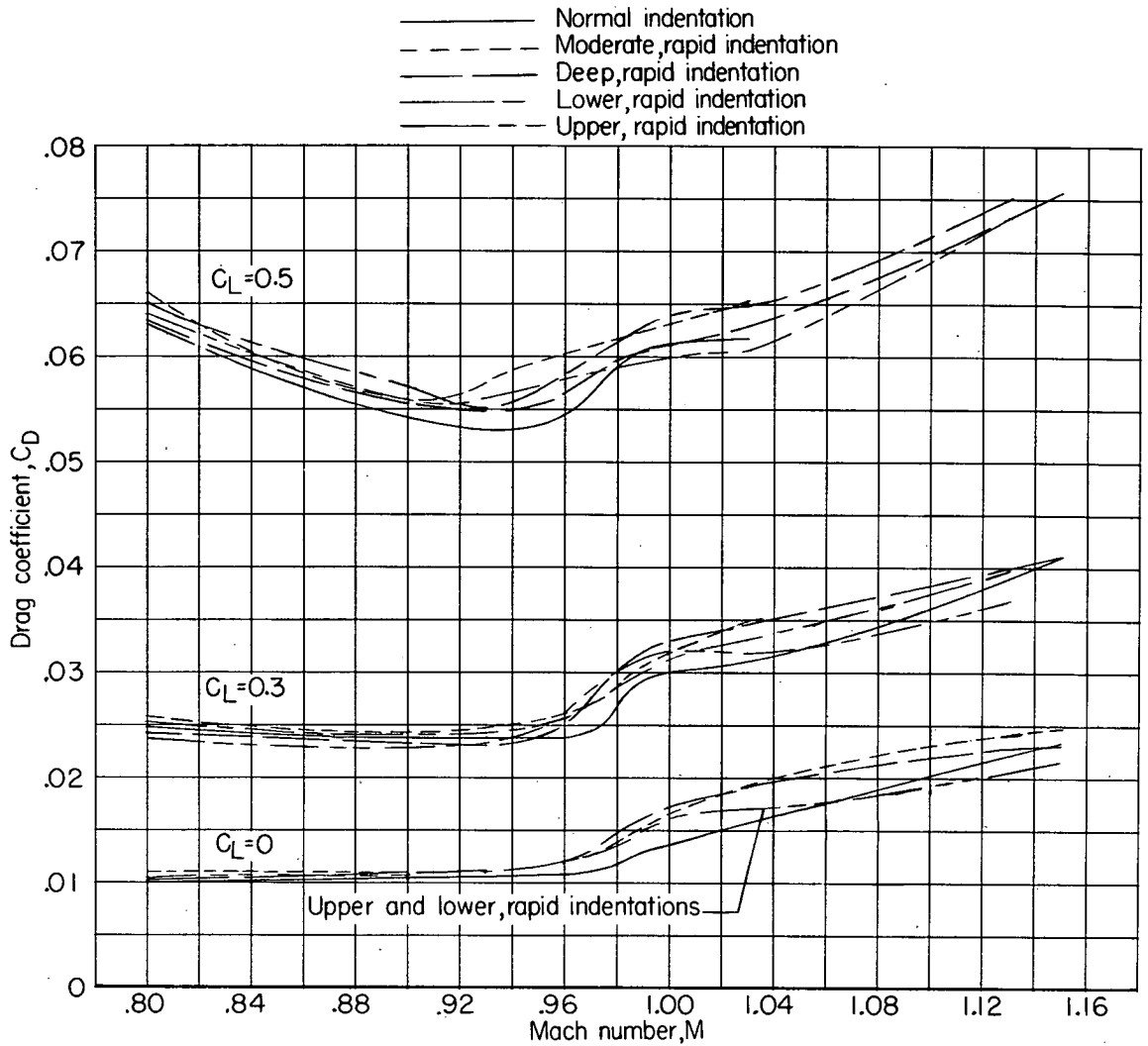


Figure 13.- Effect of increasing forward slope of normal body indentation on variation of drag coefficient with Mach number at lift coefficients of 0, 0.3, and 0.5.

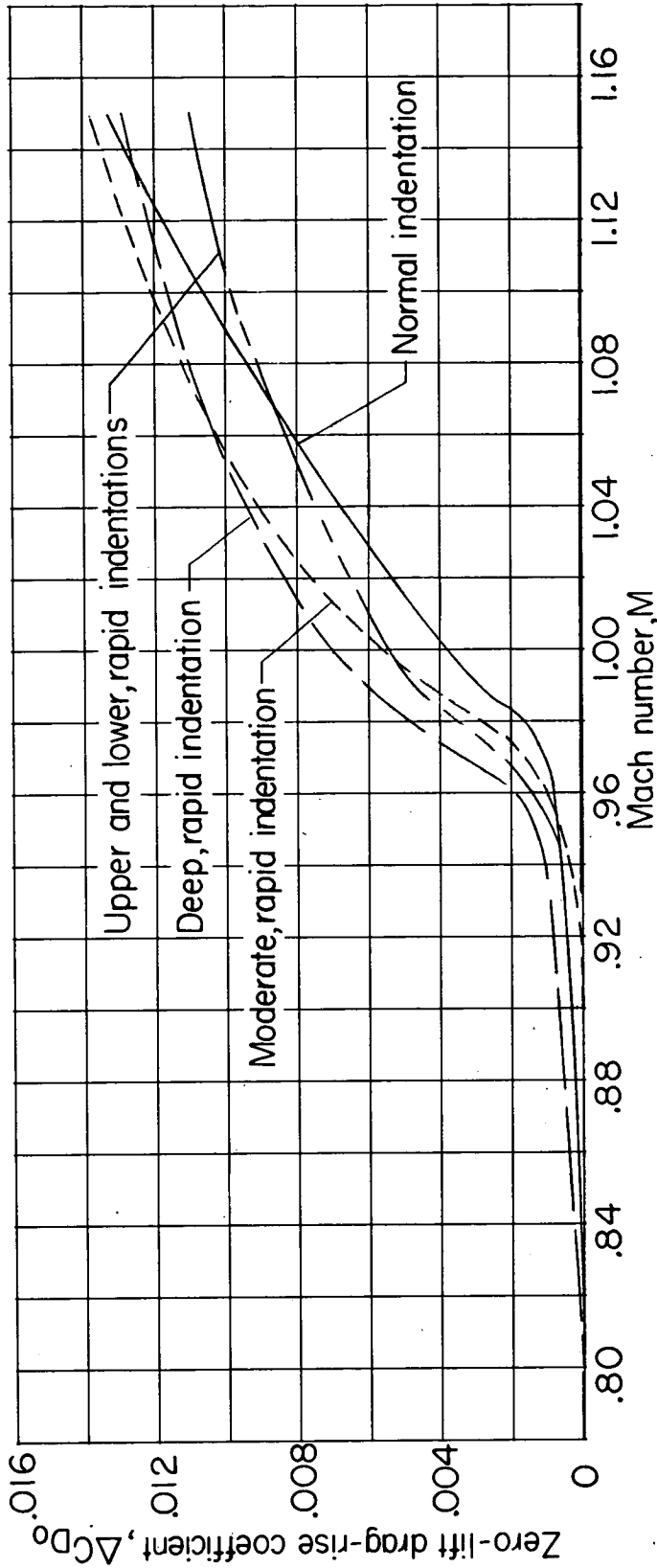


Figure 14.- Effect of increasing forward slope of normal body indentation on variation of zero-lift drag-rise coefficient with Mach number.

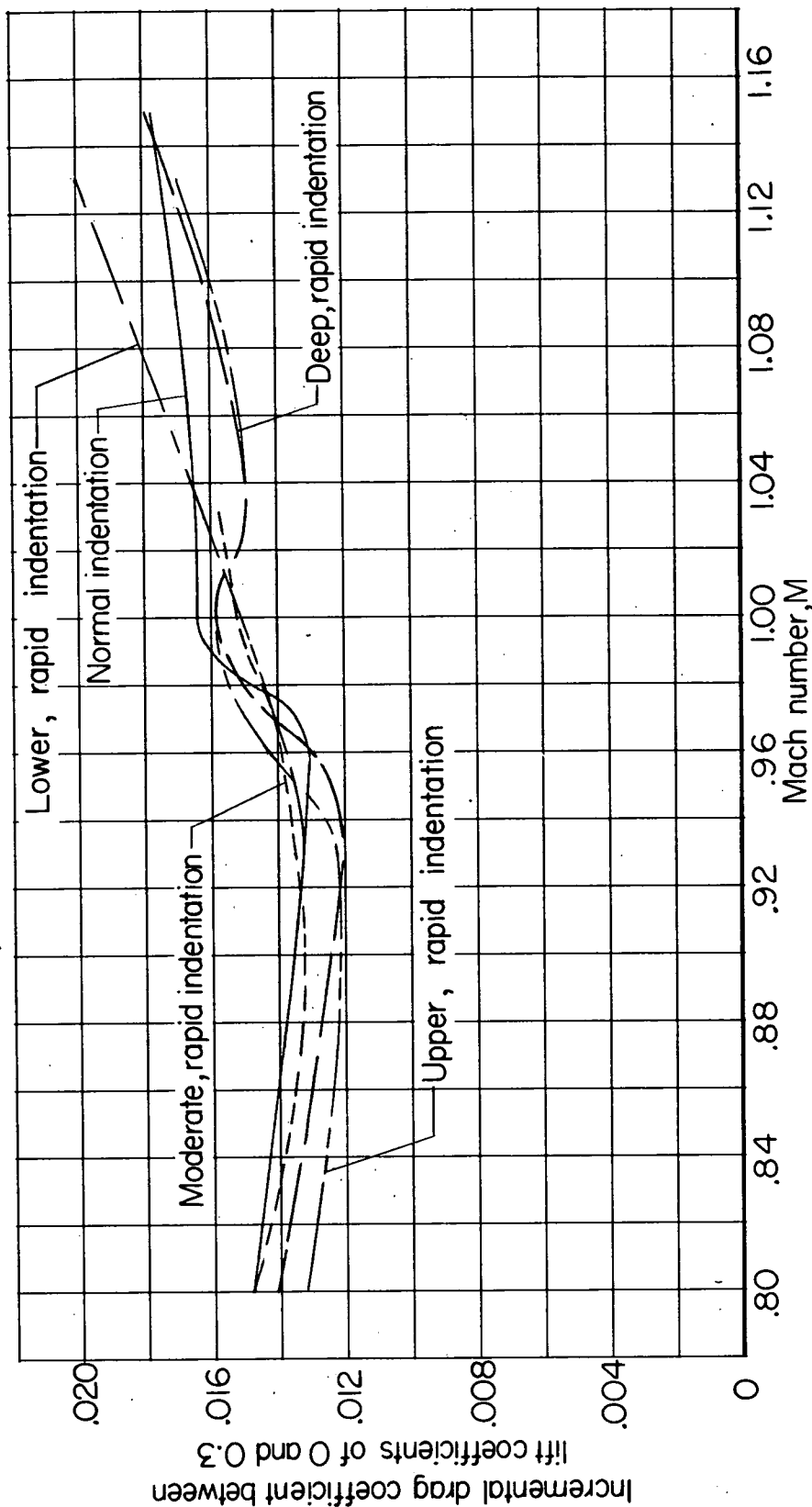


Figure 15.- Effect of increasing forward slope of normal body indentation on variation of drag due to lift at lift coefficient of 0.3 with Mach number.

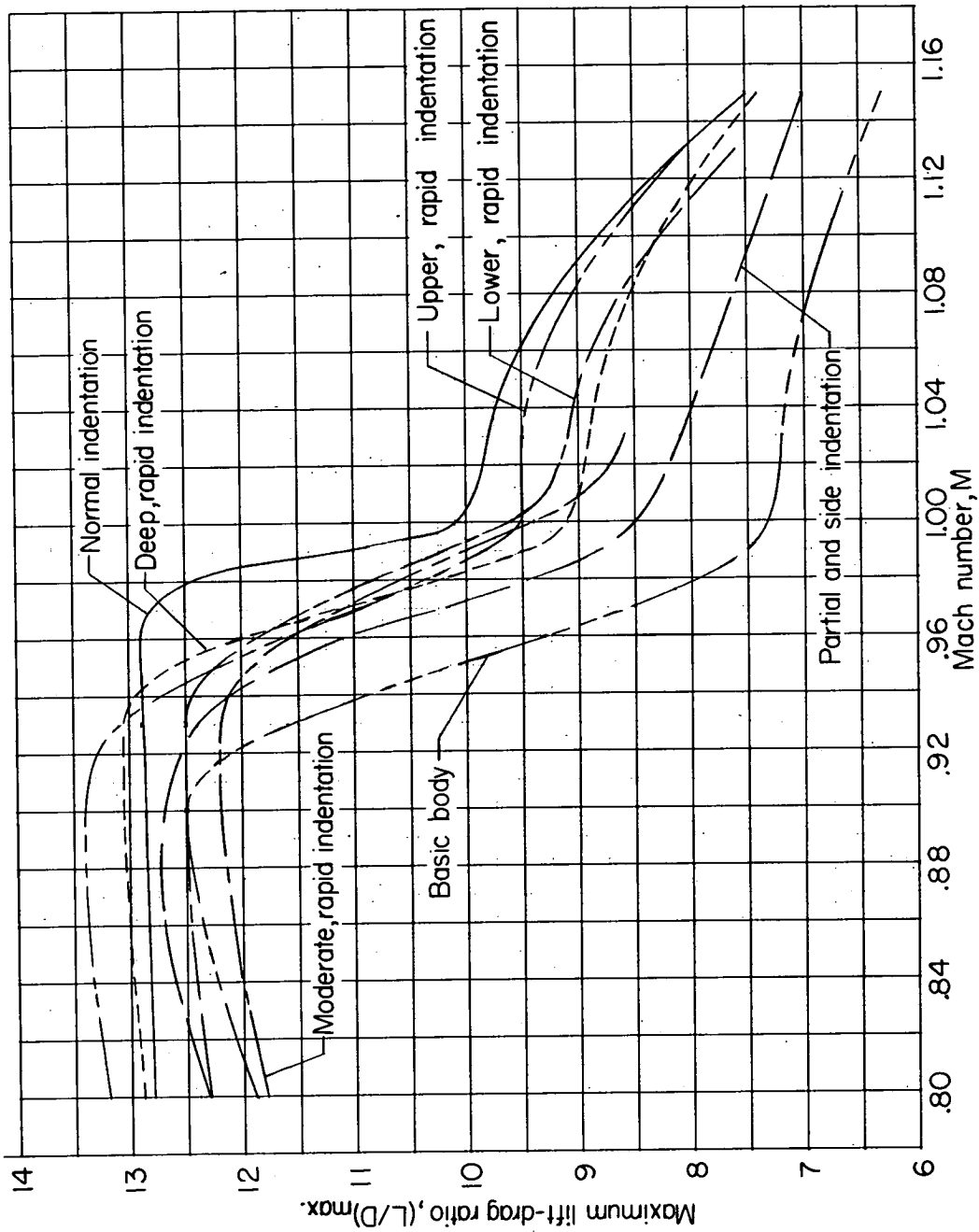
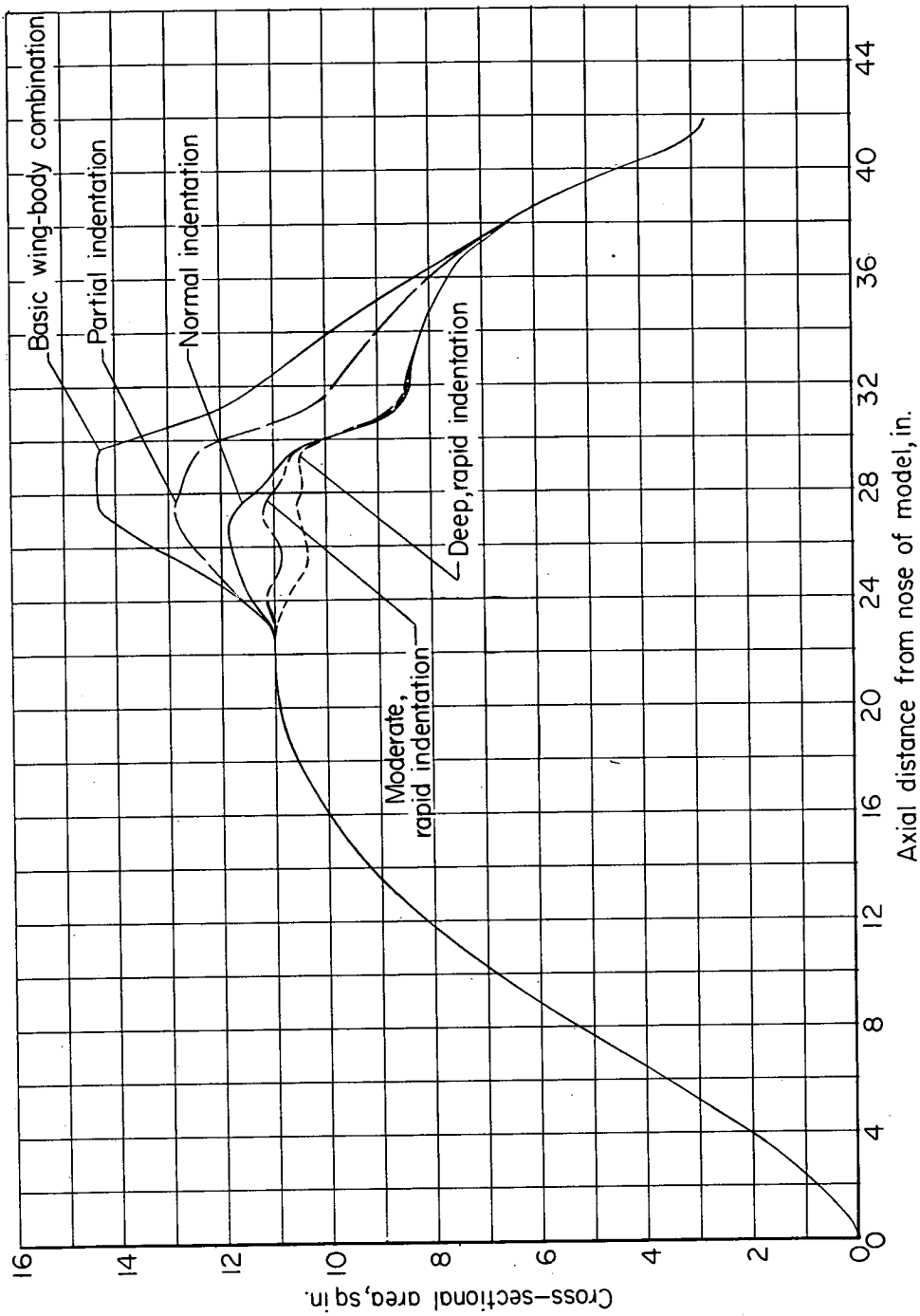
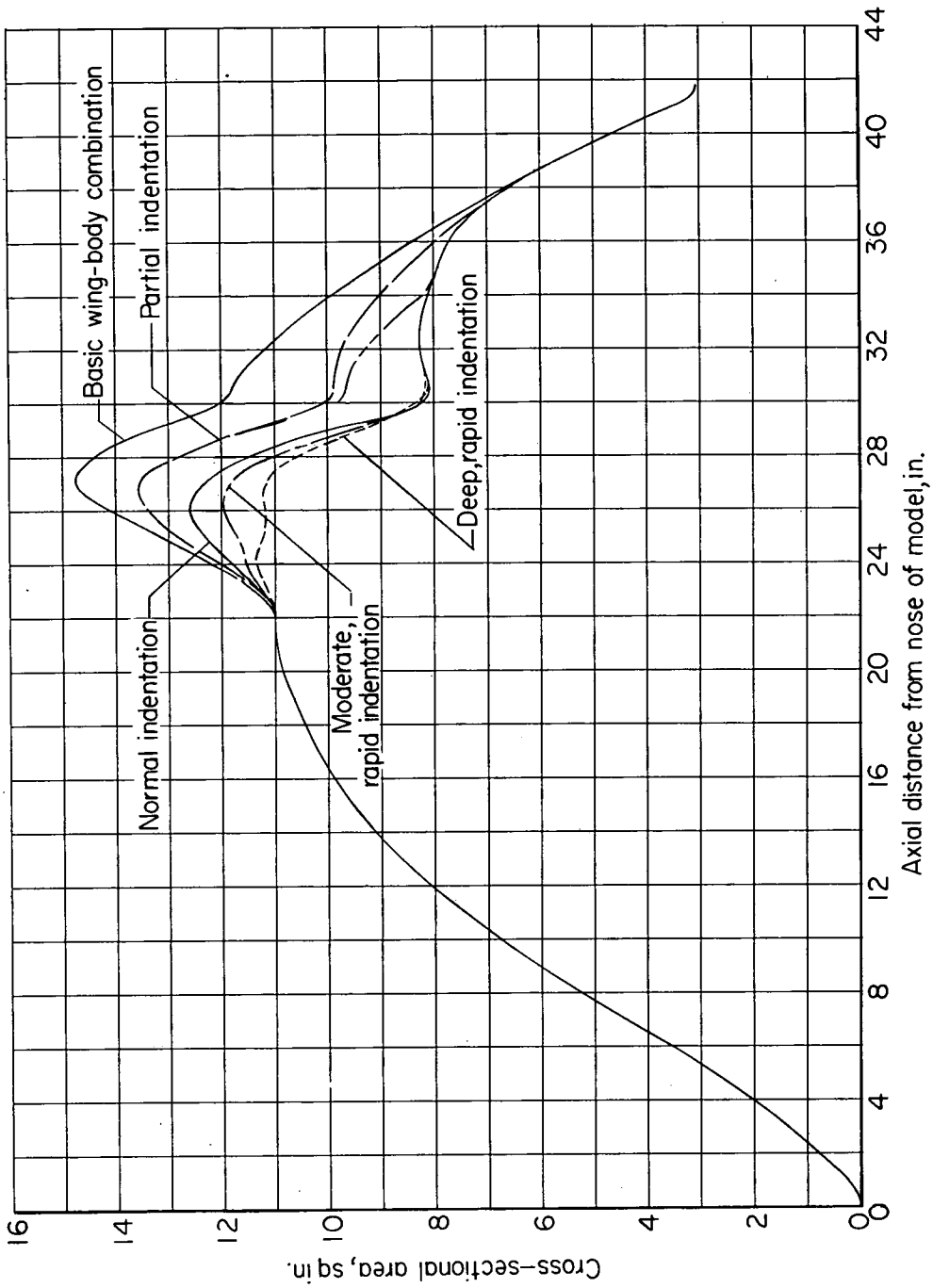


Figure 16.- Effect of several types of body indentation on variation of maximum lift-drag ratio with Mach number.



(a)  $\theta = 45^\circ$  and  $135^\circ$  for  $M = 1.20$ .

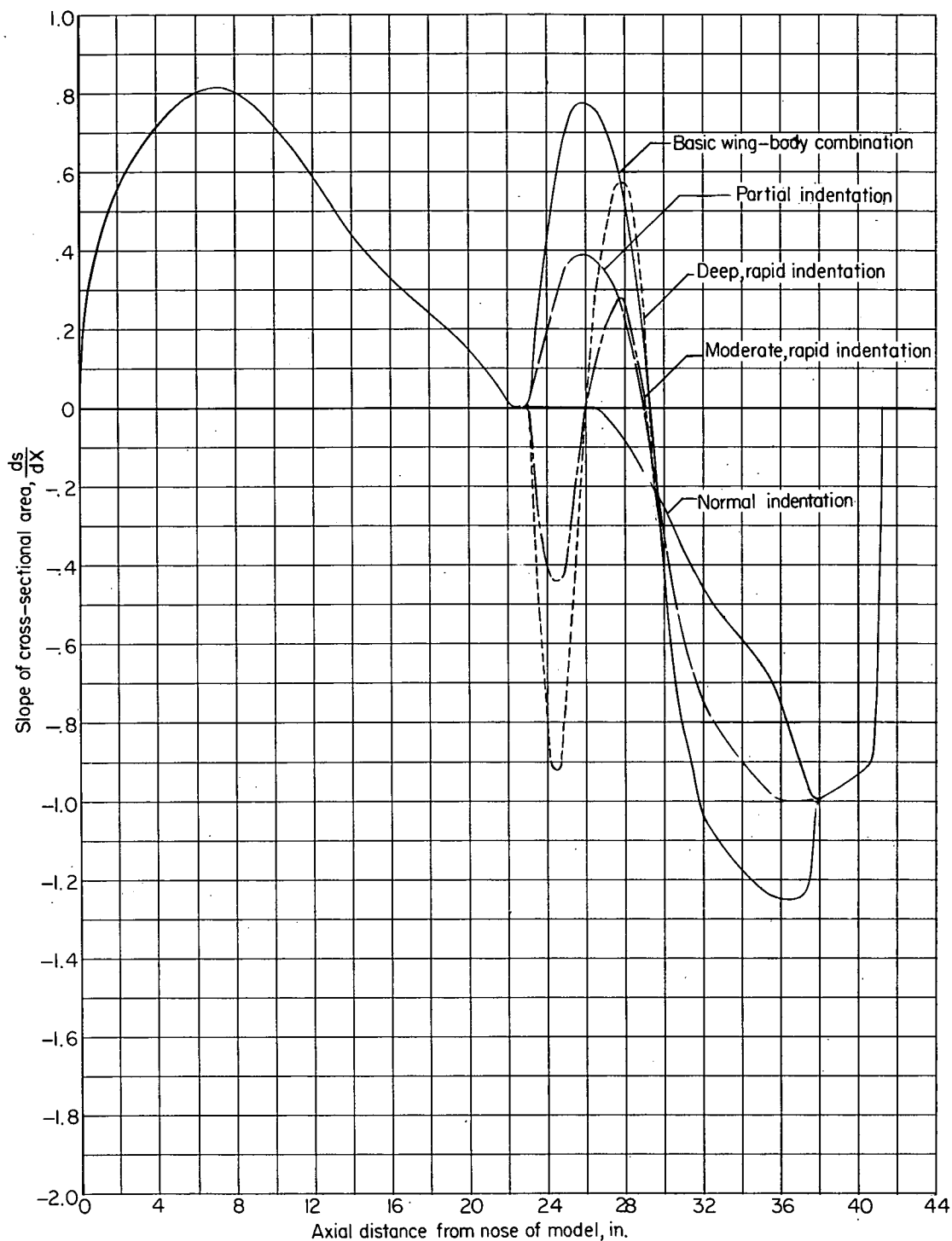
Figure 17.- Cross-sectional area distribution of wing-body combinations tested.



(b)  $\theta = 90^\circ$  for  $M = 1.20$ .

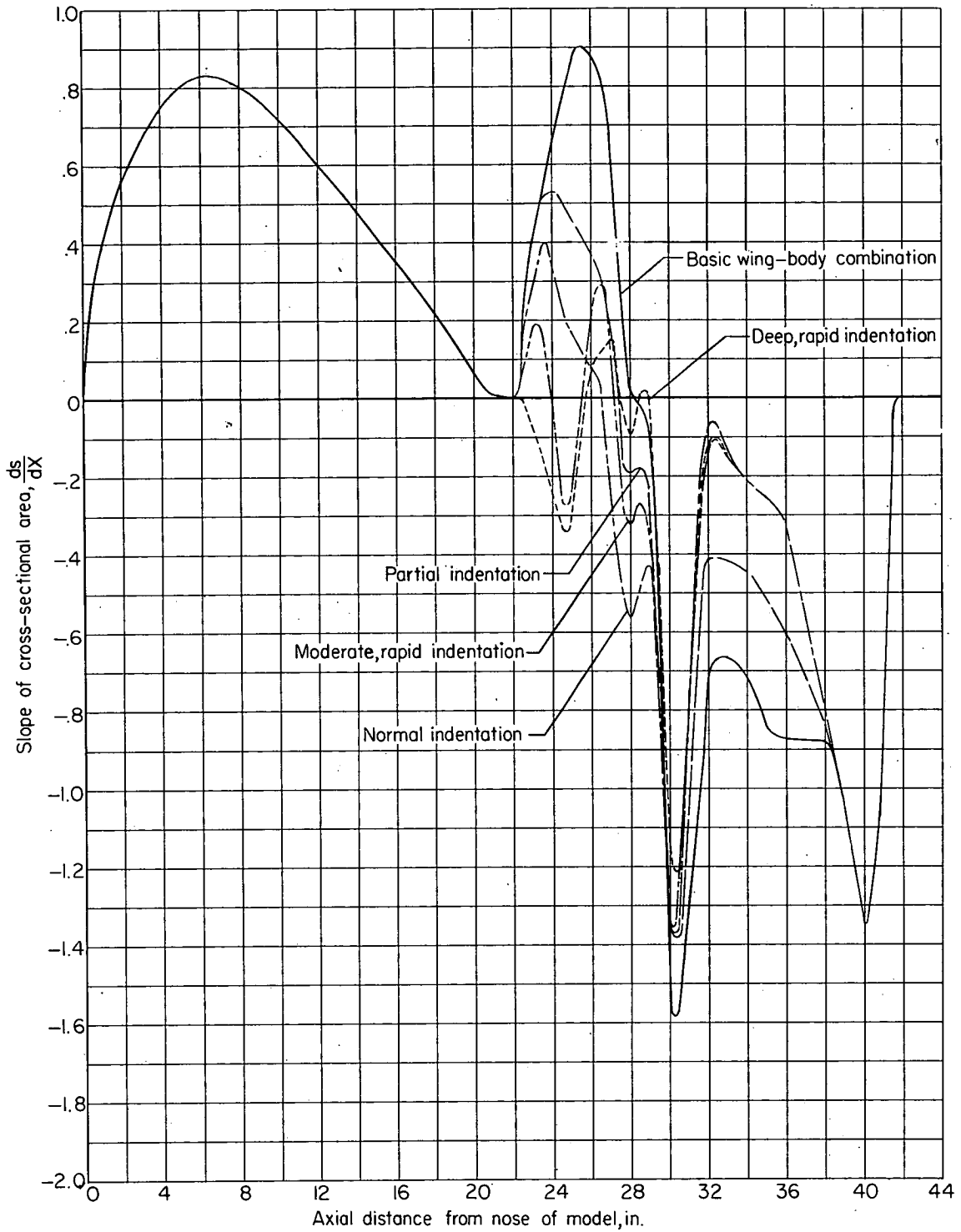
Figure 17.- Concluded.





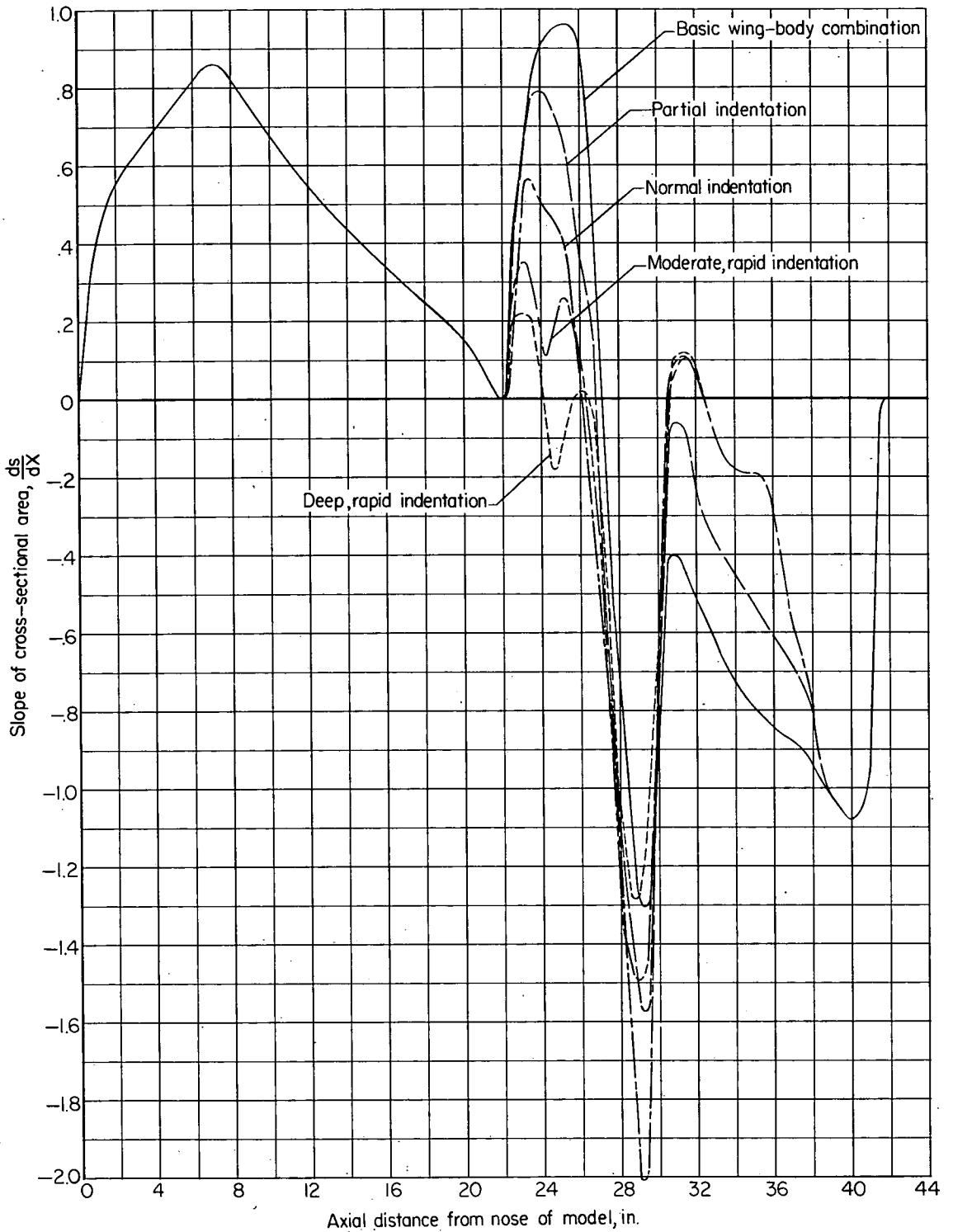
(a)  $M = 1.00$ ;  $\theta = 0^\circ$  and  $180^\circ$  for  $M = 1.20$ .

Figure 18.- Variation of the first derivative of the projected cross-sectional area with body station.



(b)  $\theta = 45^\circ$  and  $135^\circ$  for  $M = 1.20$ .

Figure 18.- Continued.



(c)  $\theta = 90^\circ$ ,  $M = 1.20$ .

Figure 18.- Concluded.

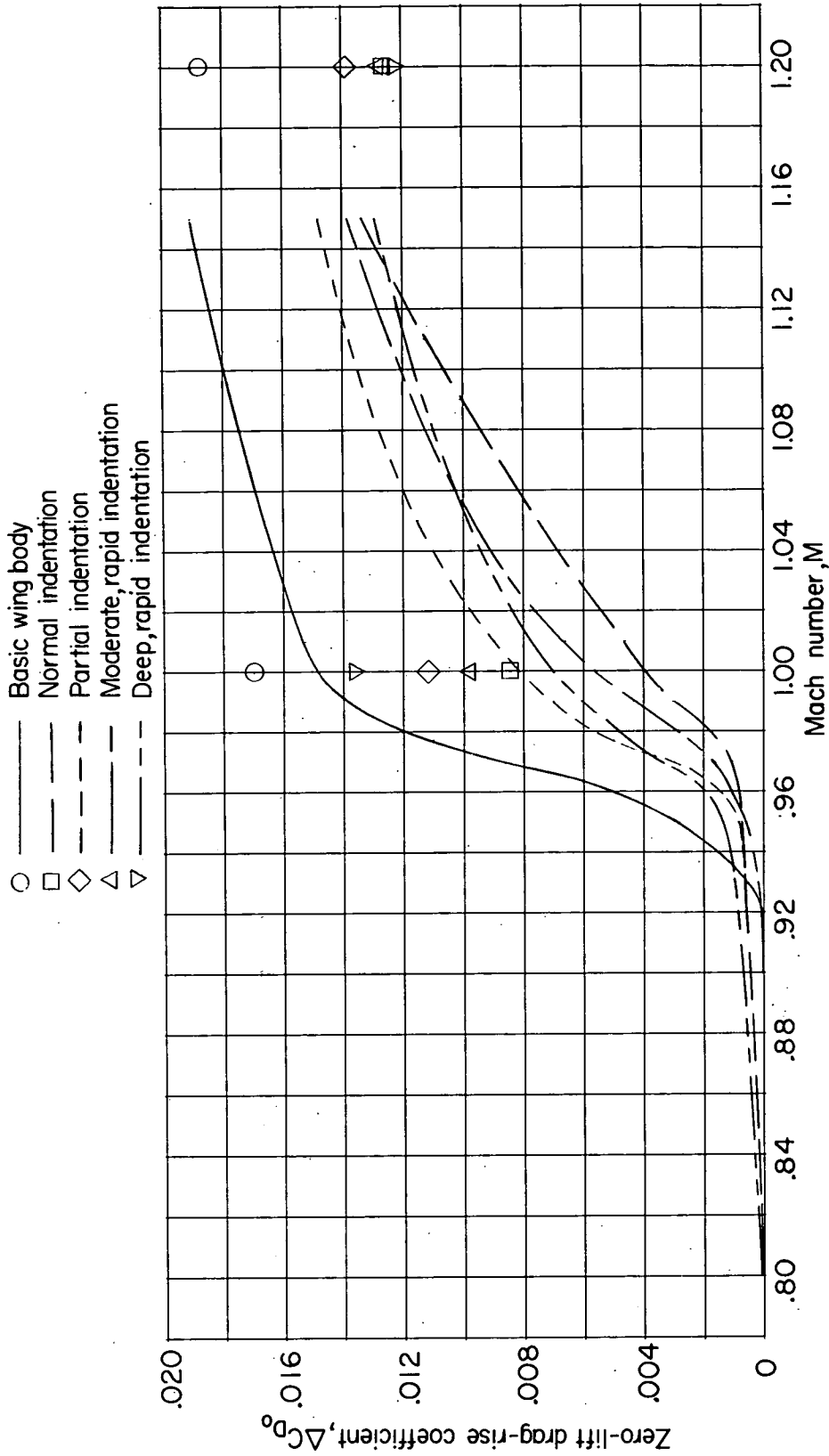


Figure 19.- Comparison of theoretical and experimental zero-lift drag-rise coefficients. (Template symbols represent theoretical data).

CONFIDENTIAL

CONFIDENTIAL